JOURNAL OF GEOPHYSICAL RESEARCH, VOL. 100, NO. C3, PAGES 4653–4672, MARCH 15, 1995

A numerical model of Arctic leads

Lakshmi H. Kantha

Department of Aerospace Engineering Sciences and Program in Atmospheric and Oceanic Sciences, University of Colorado, Boulder

Abstract. Arctic leads are thought to play an important role in the air-sea heat exchange at high latitudes. The evolution of the local ice-ocean-atmosphere coupled system, when a lead opens up and immediately begins to refreeze, is of considerable interest in terms of the heat exchanged by the ocean to the atmosphere, as well as the amount of salt extruded into the oceanic mixed layer. Here we will present a coupled model of the ice-ocean system that provides a quantitative description of a refreezing lead, especially the evolution of the ice cover and the mixed layer below. The model is applied and compared with what has been learned from the Lead Experiment (LEADEX) observations in the April of 1992 in the Beaufort Sea. The results suggest that Arctic leads, especially during winter, are, in general, close to a state of free convection. Strong convection driven by the extruded brine in a refreezing lead drives vigorous mixing in the mixed layer immediately below, irrespective of the advective velocity of ice. Turbulence intensities reach quite high values during the initial phases of refreezing but weaken gradually with a half-life time of about 2 days. Inertial oscillations are superimposed on the resulting currents and are especially vigorous below the mixed layer. The ice builds up to a thickness of over 12 cm in the first 24 hours in a refreezing lead, in accordance with LEADEX observations, with a significant contribution coming from frazil ice formation in the supercooled water below. Not surprisingly, since the water below is at or close to freezing, advection of water masses past the lead due to ice motion or prevailing currents does not alter the refreezing rate substantially, even though the frazil ice contribution shows a significant increase. Advection does affect the local properties in the mixed layer immediately below and downstream of the lead. For example, the increase in salinity, an indicator of the intensity of the refreezing process in a lead, depends very much on the motion of ice cover relative to the underlying water. For large advective velocities the salinity increase is an order of magnitude smaller than the purely convective situation and the turbulence is dominated by that generated by shear underneath the rough ice, upstream of the lead which tends to mask that generated by convection in the lead itself. For a stationary lead, refreezing gives rise to an inward jet underneath the ice and outward flow at the base of the mixed layer. Vertical motion is in the form of convective cells centered at the lead edges.

1. Introduction

The polar ice cover is an important component of the global climate system. The sea ice covers in the Arctic and around the Antarctic play a particularly important role in air-sea exchanges in polar regions on a wide range of timescales. Leads in the Arctic pack ice, those "cracks" in its ice cover, constitute only a few percent of the surface area of ice, yet it appears that the heat flux from the ocean to the atmosphere through these leads during winter is of comparable magnitude to the heat flux through the rest of the ice cover [*Maykut*, 1978]. This is simply because the very thin layer of ice in a refreezing lead exposes the relatively warm waters below to the cold atmosphere above, leading to a large heat loss from the ocean, until the ice grows thick enough to effectively reinsulate the ocean or the lead closes up. The heat flux through a lead has been estimated to be 2 orders of magnitude larger than in the surrounding pack ice [*Smith et al.*, 1990]. Most of this heat loss comes from the latent heat release from ice formation in the oceanic mixed layer underneath. The air-sea temperature difference often exceeds 40°C and therefore the heat loss, especially in the early stages when the lead opens up, is estimated often to reach magnitudes of 800 to 1000 W m^{-2}, one of the highest heat loss rates observed in the global oceans. Similar heat losses occur at the ice edges in marginal ice zones during off-ice wind conditions [*Muench et al.*, 1991]. The only events that rival these in midlatitudes are the cold air outbreaks along the east coasts of continents during winter, which also lead to air-sea temperature differences of a few tens of degrees and hence similarly large heat exchange rates that often lead to explosive cyclogenesis [*Doyle and Warner*, 1990; *Hadlock and Kreitzberg*, 1988].

Since the water masses immediately below a refreezing lead are at or close to the freezing point, the only way the ocean can provide such large heat to the atmosphere is through latent heat release from phase conversion. Ice therefore forms at a rapid rate, both as sheet ice near the surface, as well as frazil ice in the water column. Frazil ice eventually ends up near the surface. In any case the ice formation leads to considerable brine rejection, even though the ice salinities in a lead are typically higher than those even in a first-year ice. This, in

Paper number 94JC02348.
0148-0227/95/94JC-02348$05.00

turn, leads to vigorous convective mixing in the mixed layer below, leading to a local modulation of the mixed layer depth, as well as circulation. For example, under pure convection beneath a stationary ice pack, lead-driven convection leads to inward flowing jets near the undersurface of the pack ice to compensate for the outflow of the extruded brine near the base of the mixed layer [*Morison et al.*, 1992]. If the pack ice is moving, then the resulting currents tend to dominate the circulation pattern. In addition, vigorous inertial motions can be induced in the upper layers on timescales of a day or more. It is therefore of interest to simulate the circulation in the mixed layer in and around a lead, using a realistic model of the mixing driven by salt extrusion.

Leads are, by nature, transient features. This is what has made them especially difficult to observe and understand. It is the differential motion of ice cover, more precisely ice divergence, that leads to the fracture of an ice floe and opening up of a lead. Strong, transient storms passing over the ice cover result in the formation of an extensive field of leads. The lifetime of leads is typically measured in hours to days. From the very time an Arctic lead opens up during winter, physical processes conspire to close it; either the refreezing process eventually builds up a thick ice cover in the lead that reinsulates the underlying ocean or the shifting motion of the surrounding pack ice closes the lead, resulting in the formation of an ice ridge or a rubble field. Either way, the lead does not last long; yet during its short life span the ocean underneath loses considerable heat to the atmosphere above. It is for this reason that the evolution of an Arctic winter lead (and a field of leads) is of considerable interest to the thermodynamic interaction of the polar oceans with the atmosphere. A numerical study of the atmospheric boundary layer over a lead using the large eddy simulation approach to turbulence closure has recently been made by *Glendening and Burke* [1992].

During spring and summer, also, leads play an important role in the thermodynamics of the air-sea exchange. Because of the much smaller albedo of the water surface and the thin ice in the leads, the heating of the underlying ocean once again takes place preferentially through the leads. While melt ponds do decrease the effective albedo of the once snow-covered pack ice, the heating of the ocean through the thick ice cover is generally an order of magnitude smaller. Most of the solar heat input ends up in melting the top layers of pack ice, with only a fraction penetrating deep enough to heat the mixed layer below. In regions of perennial ice cover, as in the central Arctic basin, melting is therefore typically around and near the edges of the pack ice, in the leads surrounding them.

Leads are essentially small-scale features in an extensive polar ice cover. They range in width anywhere from several tens of meters to a few kilometers. Their length ranges from several hundred meters to a few tens of kilometers. They are therefore essentially linear features, in marked contrast to polynyas. Unlike polynyas, which are kept open for a long time by ice divergence or winds, leads are essentially transient features with lifetimes measured often in hours, but more typically in days. It is therefore not surprising that very few in situ observations are available, especially of winter Arctic leads. They are difficult to observe and study. An alternative means of study is through numerical modeling of the dynamical and thermodynamic processes in and around leads. The hope is that a comprehensive and reliable numerical model of the coupled ocean-ice-atmosphere around a lead can shed some light on the physical processes occurring around a refreezing lead, especially when used in concert with the few existing observations from the 1974 Arctic Ice Dynamics Joint Experiment Lead Experiment [see *Paulson and Smith*, 1974], the 1976 Arctic Mixed Layer Experiment [see *Morison*, 1980], and the more recent 1992 Lead Experiment (LEADEX) expedition [*LEADEX Group*, 1993].

Recent reviews of sea ice processes and their importance to global climate are given by *Untersteiner* [1986], *Smith* [1990] and *Barry et al.* [1993]. An excellent review of the physical processes in and around leads and polynyas has recently been provided by *Smith et al.* [1990]. This review deals primarily with the observational database that existed at the time. The reader is also referred to *Morison et al.* [1992], who provide an overview specifically of the physical oceanography of winter leads and include a simple numerical model of convection in a lead. *Smith and Morison* [1993] present the results of a more comprehensive multilevel numerical model of haline convection in leads. However, there is, as yet, no numerical model of the coupled ice-ocean system in and around a winter lead. This paper addresses that issue. Also, since brine-driven turbulent convective processes are of such importance to the evolution of a lead, it is essential to parameterize the turbulent mixing in the mixed layer underneath as accurately as possible. The model presented here incorporates a higher-order turbulence closure model to more accurately model the convection and shear-driven turbulent mixing in the mixed layer in and around a winter lead and takes into account the formation of frazil ice as well. Unlike earlier modeling studies, the timecale of the ice buildup is also investigated through multiday simulations. The disparity in the roughness of the ice undersurface in and around a lead is explicitly taken into account in the heat, salt, and momentum exchanges occurring at the ice-ocean interface.

LEADEX 1992 [*LEADEX Group*, 1993] was conducted toward early spring (not exactly under winter conditions of large air-sea temperature differences and no short-wave solar heating) when there was significant short-wave solar radiation and when the air temperatures were higher than normal, at an average value of -19°C rather than around -40°C [*Muench et al.*, this issue]. This explains the lower than normal values of heat fluxes observed. Nevertheless, the ice growth rates reached values of up to 12 cm d^{-1}. Two leads were particularly well measured, leading to a better understanding of processes in and around leads. We will simulate these leads with the numerical model in an attempt to further improve our knowledge of a refreezing Arctic lead. Simulations will also be done on leads cases studied by other modelers in the past.

The paper is organized as follows. In section 2 we review some salient aspects of circulation under leads. Section 3 contains a description of the present status of the numerical models of Arctic leads. A brief summary of the modeling efforts up to the present, concentrating on their achievements and shortcomings, is presented. Next in section 4 we describe a numerical model of the coupled ice-ocean system in an Arctic lead, and we present some simulation results in section 5. Finally, we conclude with some recommendations for improvement of lead models in view of the current study and the recent findings from the 1992 LEADEX experiment [*LEADEX Group*, 1993].

2. Some Aspects of Circulation in a Lead

Morison et al. [1992] present a comprehensive review of lead processes as known prior to the LEADEX program and provide an excellent summary of many salient features of lead-induced circulation. Here we attempt to clarify a few of those.

Since *Kozo* [1983], there has been an attempt to classify the convection under a refreezing lead into free, mixed, and forced convection cases. *Morison et al.* [1992] devote considerable effort toward the scaling arguments. By scaling the governing equations, they arrive at a lead number L_0, to characterize the nature of flow in a lead. They define L_0 as

$$L_0 = \frac{qd}{U u_*^2}, \tag{1}$$

where q is the buoyancy flux due to the salt flux produced by freezing, d is the mixed layer (ML) depth, U is the ice velocity, and u_* is the friction velocity ($u_* = C_D^{1/2}\, U$, where C_D is the drag coefficient). This number is the ratio of the pressure gradient term to the shear stress term in the momentum equation. It is also proportional to the ratio of the ML depth to a Monin-Obukhov length scale. However, u_* in (1) refers to the rough ice outside the lead, not the local value corresponding to smoother lead ice inside, while q refers to the salt flux in the lead itself. Therefore it is a parameter that also contrasts the mixing levels inside and outside the lead.

When the local value of u_* is used, L_0 is proportional to the cube of the ratio R, which is simply the ratio of the convective velocity scale w_* to the friction velocity u_* in the mixed layer, where $w_* = (qd)^{1/3}$. The parameter R is indicative of the relative magnitudes of the intensities of free and forced convection in a convective boundary layer (BL) and has been used extensively by atmospheric scientists to characterize turbulence in an inversion-capped convective atmospheric boundary layer (ABL). It is well known that surface layer similarity relations do not hold in the bulk of the convective ABL; instead, the appropriate scaling parameter for turbulence characterizing the ABL is the convective scale w_*. Since the situation in a convecting lead is somewhat analogous to an inversion capped ABL, the lead number could be defined by R, although L_0 is related to R. The lead number would then be a parameter that characterizes the nature of turbulent mixing in the mixed layer immediately underneath the lead. While the quantity U is readily measured, q and u_* are not, and there is no advantage to using L_0, instead of R, to characterize the mixing in a lead.

There is one salient difference between the ML under a lead and an ABL, which is horizontal spatial inhomogeneity. Nevertheless, if one uses average values for the "internal" BL that develops under a lead when the ice is in motion, then the parameter R can still be used to characterize the nature of turbulent mixing in a lead. It is also possible to use R_R, defined with u_* appropriate to the rough ice outside the lead (u_*^R) to contrast the turbulence level immediately underneath a lead to that outside, provided shear generation of turbulence in the lead itself is ignored. *Morison et al.* [1992] define their lead number L_0 using u_*^R, and therefore their L_0 can also be regarded as a parameter that contrasts the level of mixing inside the lead to that outside.

Another argument in favor of the use of R to characterize the nature of mixing in a lead is as follows. The characteristic turbulence velocity in the atmospheric ABL scales as (see evidence quoted by *Moeng and Sullivan,* [1994])

$$w_m^3 = w_*^3 + 5u_*^3$$

The ratio w_m/u_*, which determines if the ABL is convectively driven, shear-driven, or both is

$$w_m/u_* = (5 + R^3)^{1/3} \tag{2}$$

For $R \sim 1$, $w_m/u_* \sim 2$, and therefore this is a reasonable value to indicate the demarcation between convective and shear-driven turbulence. For $R < 1$, shear-generated turbulence dominates the mixed layer as a whole, while for $R > 1$, turbulence in the bulk of the mixed layer is convection driven. For values of R around 1, one gets mixed convection.

With this information it is easy to show that a winter Arctic lead is seldom in the forced convection regime, as far as the nature of turbulent mixing is concerned, even for a shallow mixed layer under a lead in the late stages of freezing and with a substantial ice drift. However, this is not to say that the flow pattern may not be dominated by ice motion or the turbulence outside may not be as strong as that inside. Parameter R_R defined with u_*^R would be a better indicator of these aspects.

In order to do this, we will use the *Anderson* [1961] formula for ice growth rate (in meters per second)

$$\dot{h} = \frac{B_2\, \Delta T}{(2h + B_1)} \tag{3}$$

where B_1 and B_2 are constants ($B_1 = 0.05$ m, $B_2 = 7.75 \times 10^{-9}$ m s^{-1}), h is the ice thickness in meters, and ΔT is the water-air temperature difference. For a ΔT of 15°C this formula yields an ice growth rate of 2.3×10^{-6} m s^{-1} when the lead opens up and 2.6×10^{-7} m s^{-1}, an order of magnitude less, when the lead is somewhat mature, with an ice thickness of 20 cm. These values are a few tens of a percent higher than *Maykut*'s [1978] formula would yield [see *Morison et al.*, 1992], but since it is not clear which formula is more reliable, we have just used the simpler of the two. Since R is proportional to the cube root of the buoyancy flux and hence the ice growth rate, the quantitative difference between the two formulas is about 10% or so. Note that using a value of 3.35×10^5 J kg^{-1} for the latent heat of fusion, a typical heat loss rate of 600 W m^{-2} when a lead opens up initially, yields an ice growth rate of 1.7×10^{-6} m s^{-1}, while at the mature stage, the heat loss drops to levels of about 100 W m^{-2} or less, leading to growth rates of 2.9×10^{-7} m s^{-1}. These values are not very far from those obtained above using *Anderson*'s [1961] formula.

The corresponding salt flux (F_s) is given by

$$F_s = \frac{\rho_i}{\rho_o}(1 - k_c)\, S_w \dot{h} \tag{4}$$

where k_c indicates the fraction of salt retained in the lead ice. The quantities ρ_o and ρ_i denote the density of water and ice respectively and S_w is the salinity of water. While the freshly formed ice is quite salty (values up to 25 practical salinity units (psu) have been observed during LEADEX), k_c seldom exceeds 0.5 and is usually in the range of 0.3-0.5 [*Morison et al.*, 1992]. Using the highest possible value of 0.5 to get the weakest convection possible and S_w of 32 psu (a typical value for the mixed layer salinity), the buoyancy flux in a lead can be written as $q = 0.109\, \dot{h}$ m^2 s^{-3}, where $\dot{h}$ is the ice growth rate in meters per second. Therefore the convective velocity scale is

$$w_* = 0.48\left(\dot{h}d\right)^{1/3}, \tag{5}$$

where d is the mixed layer depth in meters.

Using a value of 10 m for d, indicative of a rather shallow mixed layer, and $\dot{h}$ of 2.6 x 10^{-7} m s^{-1} corresponding to a lead covered already with a 20-cm thick ice cover, we get $w_* = 0.66$ cm s^{-1}. (For a freshly opened lead, with a heat loss of 600 W m^{-2} and a more typical mixed layer depth of 30 m, $w_* =$ 1.78 cm s^{-1}.)

We need to compare this to the typical value of friction velocity u_* under a lead. Recalling that the ice in a lead is usually smooth, and therefore selecting a C_D value of 0.001, u_* is 0.45 cm s^{-1} for a relatively high ice drift rate of 15 cm s^{-1}. Thus the ratio R is 1.5, indicating that free convection is more prevalent, even in this most conservative case of large ice drift, shallow mixed layer, weak convection due to maturity of the lead, and a rather modest air-sea temperature difference. For a more typical freshly opened winter lead, with heat losses exceeding 1000 W m^{-2} and a mixed layer depth of 30 m, w_* is likely to exceed 2 cm s^{-1}, while u_* is likely to be less than 0.3 cm s^{-1} for typical ice drift velocities of 10 cm s^{-1} or less, thus leading to an R value of nearly 7. Thus free convection is likely to dominate mixing under a winter lead more often than not. At best, mixed convection can result, but forced convective limit is seldom realized.

Kozo [1983] used a value of 1.25 cm h^{-1} for ice growth rate in his simulations and assumed a value of 0.3 for k_c. This leads to a value of 2.7 cm s^{-1} for w_* for his mixed layer depth of 35 m. This is quite a strong convective situation, since in his simulations, the ice velocity has a maximum value of 5 cm s^{-1}, leading to a u_* of 0.15 cm s^{-1} at best. The ratio R is therefore 18, indicative of the fact that convective turbulence clearly dominates his simulations.

Morison et al. [1992] used a value of 600 W m^{-2} for the heat loss in their simulations, equivalent to a growth rate of 0.625 cm h^{-1}, half that of *Kozo* [1983]. With $d = 40$ m and $S_W = 32$ psu, using a value of 0.5 for k_c, one arrives at a value of 2.1 cm s^{-1} for w_*. Their more realistic case 2 simulation uses a value of 0.5 cm s^{-1} for u_*, leading to a value of more than 4 for R. Clearly, convective mixing dominates, even though the lead drifts at a rather high rate of 20 cm s^{-1}, as was indeed confirmed by their simulation results.

While it is clear that immediately below a refreezing lead, convective mixing dominates, the circulation pattern behaves differently. The presence of even a small ice drift tends to overwhelm the typical free convection induced, roll-type circulation underneath the lead. This difference should be kept in mind when looking at observations and model simulations presented here. The parameter R_R, which is proportional to cube root of lead number L_0 of *Morrison et al.* [1992] could be used to determine if ice motion overwhelms the local convection.

Finally, there remains the problem of how to detect lead-induced convection to determine if the lead is "active." The most logical choice at a first glance would be the increase in mixed layer salinity brought about by salt rejection from freezing ice. However, as can be easily shown and as reflected in the simulations presented below, the salinity perturbations are usually small, unless the advective velocities are very small, thus leading to a nearly convective situation. The perturbations in turbulence intensities are, however, quite intense in most cases. Therefore as *Morison et al.* [1992] suggest, turbulent fluctuations in the mixed layer might be a better indicator of lead activity immediately underneath. Even this is not unambiguous for the case of a weakly convecting lead surrounded by fast moving rough pack ice, where the ambient turbulence levels are likely to mask those due to lead activity.

To put an upper bound on salinity perturbations to be expected in a mixed layer due to a convecting lead, consider a highly simplified box model of the lead. The box surrounds the lead, whose width is L, and extends down to the halocline at a depth of d. We will assume that the properties are uniform in the vertical in the mixed layer and the lead convection due to freezing at the rate of $\dot{h}$ m s^{-1} produces an increase of $\Delta S = (S_w - S_{w0})$ in salinity immediately underneath. The water masses are therefore advecting out a salt flux of $U \Delta S d$, where U is the advective velocity. Freezing in the lead inputs a salt flux of $\dot{h}(1 - k_c)S_w$. An equation for the rate of change of ΔS can therefore be written as:

$$\frac{\partial}{\partial t}(\Delta S) = \frac{\dot{h}(1 - k_c)S_w}{d} - \frac{U \Delta S}{L} \tag{6}$$

Two limiting cases can be considered. For pure convection, $U = 0$ and therefore

$$\frac{Sw}{Sw_0} = exp\left[\frac{h\ (1-k_c)}{d}\right] \tag{7}$$

Since the quantity in square brackets is small,

$$\Delta S = \Delta S_c = S_{w0}\ (1-k_c)\, h\, /\, d \tag{8}$$

For advection, if we assume that the salt put into the ML is immediately mixed through the ML, then the advective flux balances the salt flux and we get

$$\frac{Sw}{Sw_0} = \left\{1 - \left[\frac{(1-k_c)\, L\dot{h}}{Ud}\right]\right\}^{-1} \tag{9}$$

which can be simplified further

$$\Delta S = Sw_0 \frac{(1-k_c)\, L\dot{h}}{Ud}. \tag{10}$$

An exponential functional relation for h in terms of time since the lead opening is quite typical of observations

$$h(t) = h_o(1 - e^{-at}). \tag{11}$$

Typical values are $a = 8$ x 10^{-6} s^{-1} and h_o (the asymptotic value) is 0.3 m, leading to a growth rate of about 0.8 cm h^{-1} during the initial stages of the lead opening and an ice accumulation of about 15 cm in a day, values typical of those observed during LEADEX. Thus for free convection, at a point in time, when the ice has grown to a thickness of 15 cm in the lead, which is typically a day, assuming a shallow mixed layer of 10 m, $k_c = 0.5$, $S_w = 32$ psu, and $\Delta S = 0.24$ psu. This is an absolute upper bound on the salinity perturbation, since convective circulation itself will tend to bring this value down by entrainment. The actual values will therefore be somewhat less. For a more typical value of 30 m for the mixed layer depth, ΔS is reduced to 0.08 psu. Perturbations of this magnitude are quite detectable.

For the advective case the maximum value for ΔS occurs at the time of maximum salt flux, near $t = 0$

$$\Delta S = \Delta S_a \approx Sw_0\ (1-k_c)\left(\frac{h_o}{d}\right)\left(\frac{aL}{U}\right). \tag{12}$$

This is equal to ΔS_c at $h = h_0$ divided by (U/aL). Even a small advection drastically reduces the salinity perturbations, as can be seen for the case of $U/aL = 10$. For $d = 10$ m, ΔS is 0.024 psu. For a lead width L of 120 m this corresponds to a value of 1 cm s^{-1} for U. For $U/aL = 100$, corresponding to $U = 10$ cm s^{-1}, ΔS is 0.0024 psu, a value 2 orders of magnitude smaller than the free convective one. Clearly, advection greatly attenuates the salinity perturbation underneath a convecting lead.

Finally, we turn to the possibility of using turbulence levels as indicators of lead activity. The turbulence intensities immediately under a lead scale with the convective velocity w_*, as shown above, since the shear-generated turbulence is generally relatively small. However, the rough ice surrounding a lead produces intense shear-generated turbulence (convective turbulence there is negligible), which scales with u_* under the thick ice, and it is the relative magnitude of the two, the parameter R_R, that determines if the lead activity can be detected or not . Assuming a C_D of 0.0025 for the rough ice, a conservative value, $u_*^R = 0.05\ U$. For a strongly convecting lead, w_* is around 2 cm s^{-1} and assuming an ice velocity of 10 cm s^{-1}, u_*^R is 0.5 cm s^{-1} and $R_R \sim 4$. Therefore the lead activity can be detected readily from elevated turbulence intensities immediately underneath the lead. However, during mature stages of a lead, w_* is typically 0.5 cm s^{-1} or less, of similar magnitude as the $u_*^R (R_R \sim 1)$. In this case the turbulence intensity in the lead is not much different from that in the surrounding waters. Far from the lead, an elevated salinity anomaly is the best indicator of an active lead nearby, since turbulence created under the lead dies out quickly to ambient levels, even when the lead activity is vigorous.

It is therefore possible to use both the salinity anomaly and increased turbulence level immediately underneath the lead as indicators of lead activity. Away from the lead however, only salinity anomaly can be used, but, by far, the simplest would be to use the lead ice thickness; the lead activity slows down dramatically with increase in the thickness of ice cover in the lead.

3. A Review of Lead Models

There have been several noteworthy efforts to model wintertime leads [*Schaus and Galt*, 1973; *Kozo*, 1983; *Morison et al.*, 1992; *Smith and Morison*, 1993], each of which has been successful in providing some valuable insights into the physical processes in and around a refreezing lead. For recent reviews of leads the reader is referred to *Smith et al.* [1990] and *Morison et al.* [1992]. The latter provides a compact summary of our pre-LEADEX understanding of the physical oceanography of Arctic leads, both from observations and model simulations. Nevertheless, all of these efforts have tended to concentrate on the convection in the mixed layer underneath and therefore have failed to address one or another salient aspect of the coupled ice-ocean system in and around a refreezing lead.

The very first attempt at modeling lead-induced circulation by *Schaus and Galt* [1973] ignored convective effects and treated the problem as simply an advective-diffusive process. These simulations were therefore quite unrealistic. However, *Kozo* [1983] succeeded in obtaining a fairly realistic depiction of the convective processes under a refreezing lead for both purely convective, as well as advective, conditions. He used a hydrostatic model to simulate the circulation in a 120-m-wide lead, with a horizontal resolution of 15 m and a vertical resolution of 5 m and a domain of 360 m. He also explicitly included a 2.5-m thick constant stress surface layer using observations in the constant stress layer of the atmospheric boundary layer (ABL) to characterize the flux profile relationships near the ice-ocean interface. The initial density field corresponded to a water column well mixed in the upper 35 m and on the freezing line at a salinity of 31 psu (temperature of -1.5°C). The water below to 95 m bottom depth had a higher salinity value of approximately 31.7 psu, leading to a strong halocline at the base of the mixed layer. While his flux profile relationships near the surface were realistic owing to the use of the well-known ABL Monin-Obukhoff surface layer relationships, his vertical mixing coefficients in the bulk of the mixed layer were quite ad hoc, decreasing linearly to zero at the base of the mixed layer from the surface layer values for stable cases and held constant for unstable stratification.

Kozo [1983] performed simulations that lasted only 4 hours, a relatively short time in the life of many leads. He also did not compute the ice growth rate based on the thermodynamic aspects of the coupled ice-ocean system but, instead, prescribed a constant ice growth rate equivalent to 1.25 cm h^{-1}. This allowed him to prescribe a salt flux into the ocean, which, in turn, drove the circulation beneath the lead. He, however, did investigate the influence of ice motion on the circulation. Under pure convection (no ice motion) his model simulations showed inward flowing jets of a few centimeters per second underneath the ice surface, akin to those observed in the field, and a symmetric circulation in the lead. Ice drift perpendicular to the lead of even a few centimeters per second changed the circulation drastically. At a 2.5-cm s^{-1} ice drift the circulation became markedly asymmetric, with downward motion occurring at the trailing edge of the lead, instead of at the center. However, an increase to 5 cm s^{-1} very nearly obliterated the signature of free convection in the velocity field. The salinity changes in the mixed layer were qualitatively similar in all three cases, which is not very surprising because advection of water masses past the lead can not lead to significant contribution of sensible heat, since the masses are at freezing conditions. It is likely that advection could lead to marked differences if the water masses being advected past the lead were above the freezing point. Then the ice growth rate would be reduced and so would be the intensity of convection and circulation in the lead.

While *Kozo*'s [1983] study gives us very important insights into lead circulation, it suffers from significant drawbacks. Since mixing processes are so important to the coupled ice-ocean system under the lead, accurate parameterization of salt flux and advection-driven turbulence in the mixed layer underneath and around the lead is essential for a realistic depiction of the ice growth in a lead and the circulation underneath. Since the inertial period is nearly 12 hours, it is essential to perform simulations lasting at least a day to examine the spin-up of currents induced under the ice. Clearly, over such a longer duration the salt flux can not be assumed to be constant and neither can be the ice growth rate. Observations clearly show a marked decrease in the ice growth rate following the initial few hours after a lead opens up. This effect needs to be taken into account by coupling the ocean to the ice thermodynamically. Kozo also assumed salinity of the fresh ice to be 10 psu, while recent observations show that it is likely to be at least 50% higher, which would lead to weaker convection under the lead. He also assumed the lead ice to be rough with a roughness scale z_0 of 0.001 m, equivalent to roughness elements under the lead ice with a physical size of 3 cm, clearly an overestimate. However, the value of 1 cm for z_0 is not unreasonable for thick Arctic ice surrounding the lead.

Using *Kozo*'s [1983] value for the ice growth rate, it can be shown that the convective velocity scale $w_* = (qd)^{1/3}$ where q is the buoyancy flux and d is the mixed layer depth, is 2.7 cm s^{-1}, while the friction velocity, using a C_D of 0.001 appropriate to a smooth ice is only 0.15 cm s^{-1} , even at an ice drift value of 5 cm s^{-1}. Thus the ratio R is 18, indicating that his forced convection cases are actually dominated by free convection. In Kozo's simulations the ice drift velocity has to be nearly a meter per second before forced convection assumes the same importance as free convection as far as the nature of turbulence is concerned. His diffusivity values are held constant at the surface layer values, while, in reality, turbulence intensity increases dramatically in the mixed layer due to unstable stratification. It has been well known to ABL modelers [*Deardorff*, 1980] that the appropriate scaling in a convective mixed layer is w_* as given above and not the free convection scaling applicable to the constant stress surface layer, which is but a small portion of the convective ABL. Once again, Kozo's simulations underline the importance of parameterizing accurately the turbulence generated by free and forced convection, perhaps by solving the appropriate equations for the turbulence quantities in the mixed layer.

Morison et al. [1992] present a highly simplified model of lead convection, an extension of a mixed layer model by *McPhee* [1987]. They assume that the problem of a steady two-dimensional flow past a lead is equivalent to a one-dimensional, time-dependent problem and invoke a simple advective transformation to a coordinate system moving with the ice. However, this is equivalent to ignoring the all-important advective terms in the governing equations, and therefore their model is a rather idealized simulation of the actual lead problem. Also, the model is valid only for nonzero advection. They also considered a rather large lead of width 1400 m and a high drift rate of 20 cm s^{-1} and confined their simulations to a duration of 4 hours, only half of which involved freezing. Their heat loss rate of 600 W m^{-2} is equivalent to an ice growth rate of 0.625 cm h^{-1}, exactly half that of *Kozo* [1983]. It is not clear what fresh ice salinity value they used, but assuming it to be half that of water, the convective velocity scale w_* is 2 cm s^{-1}. Therefore their first case is equivalent to a mixed convection case, the lead number R being about 1.3, while their second case is closer to a free convection case, with R of 0.25. This is consistent with their results [*Morison et al.*, 1992, Figures 16b and 17b]. While their model does a good job of depicting the mixing underneath a refreezing lead, it suffers from a few drawbacks, including an unrealistic dynamical field, which, in turn, affects the salinity field. Also, perhaps owing to the turbulence scaling employed in the model, a highly statically, unstable salinity gradient develops in the mixed layer. Observations in an inversion-capped convective ABL show that the unstable gradients are generally small, since intense turbulence generated as a result of strong convection tends to keep the ABL well mixed. The same must hold in the mixed layer under a lead. The salinity perturbations depicted by the model are therefore somewhat large. Also, like *Kozo*'s [1983] simulations, there is no coupling to ice growth, ice growth rate being simply prescribed and held constant.

The most recent attempt at simulating the haline circulation in and around a lead is that of *Smith and Morison* [1993]. They have applied a two-dimensional version of the Geophysics Fluid Dynamics Laboratory (GFDL) Z level, rigid lid model [*Pacanowski et al.* 1991] to simulate the circulation underneath a 750-m-wide lead. The mixed layer is 50 m deep, and the bottom depth is 100 m. The resolution is the same as *Kozo*'s [1983], 5 m in the vertical and 15 m in the horizontal. The domain width is 2250 m. The fluid below the mixed layer is stably stratified. Following *Pacanowski and Philander* [1981], oceanic mixing is parameterized using a Richardson number dependent diffusion coefficient. Surprisingly, they choose not to incorporate convective overturning in the water column by either convective adjustment schemes often employed in GFDL-type models or large mixing rates typical of strong convective processes. The resulting turbulent mixing in and around the lead are grossly underestimated, and this might have had a significant influence on the circulation reported.

The equation of state is also considerably simplified in the *Smith and Morison* [1993] model and is a function only of the salinity. The salt flux is prescribed and held fixed during the model simulation and corresponds roughly to the situation when a lead opens up and the air temperature is about -20°C. There is no coupling to ice growth; instead, an effective ice growth rate is prescribed, about 1.1 cm h^{-1} in this case. A unique feature of this model is that the lead is advected in the domain through a quiescent ocean. This technique facilitates visualization of spectacular internal wave motions generated by the dense brine plumes shed at the edges of the lead.

Smith and Morison [1993] simulations are primarily for the purely convective case of zero lead advection, which leads to symmetric circulation, and the advective case with a velocity of 5 cm s^{-1}, where the plumes are shed at the trailing edge. Both lead to generation of internal waves at the base of the mixed layer. These simulations are the very first ones to extend over several inertial periods. While they provide valuable insight into episodic plume shedding and internal wave generation by lead circulation, they do suffer from inaccurate simulations of turbulent processes in the mixed layer. It is not clear how their results, including the highly sensitive process of episodic plume shedding, would be affected by a more realistic depiction of mixing and coupling to ice growth.

4. Methodology

With a view toward alleviating some of the problems of earlier lead simulations we have made some simulations of the ice-ocean system in and around winter leads, using a more realistic numerical model of the lead-driven circulation. Leads are pretty much linear features, and therefore a two-dimensional model depicting a vertical section perpendicular to the lead axis is a good approximation. As a step toward a fully coupled model of the ocean-ice-atmosphere system, we present here a two-dimensional ocean-ice coupled model that enables us to investigate the evolution of the coupled ice-ocean system in and around a lead.

The ocean circulation model includes a second-moment closure for turbulent mixing based on the approach of *Mellor and Yamada* [1982] and *Galperin, Kantha, Hassid and Rosati* [1988] (see, also, *Kantha and Clayson* [1994]). The closure involves solving a two-equation turbulence model for turbulence length and velocity scales and parameterizing the mixing coefficients in terms of these scales using quasi-equilibrium approximation. The mixed layer depiction is therefore expected to be quite realistic. Secondly, the ocean is coupled to the ice, both thermodynamically and dynamically, using the ice-ocean coupled model described by *Kantha and Mellor* [1989], *Mellor and Kantha* [1989], *Häkkinen, Mellor, and Kantha* [1992], and *Häkkinen and Mellor* [1992]. For most of the details of the ice-ocean coupled model the reader is referred to *Kantha and Mellor* [1989] and *Mellor and Kantha* [1989]. Here we will present only the modifications to the original model.

The ice dynamics is much simplified by assuming the ice cover to be full (ice concentration of unity everywhere) and immobile (zero relative ice motions, no internal ice stresses). The coordinate system is fixed to the ice, and the water masses are advected past the lead as in the simulations by *Kozo* [1983] and unlike the *Smith and Morison* [1993] model. We expect that the improved depiction of mixing and coupling to the ice will provide for a more realistic simulation of the lead-driven circulation than has been possible thus far.

Whereas the surrounding pack ice undersurface is rather rough and might consist of extensive pressure ridges, the sheet ice formed in the lead is quite thin and easily deformed. Often, lead ice is broken up and rafted. Nevertheless, it is still considerably smoother than the surrounding pack ice. It is therefore important to take this disparity into account when considering the shear-driven turbulent mixing and heat and mass exchanges that occur when the ice is in motion. We use *Yaglom and Kader*'s [1974] formulation for both lead ice and rough pack ice surrounding the lead, but the rough ice is taken to have a roughness scale z_0 of 0.01 m, corresponding to roughness elements of about 30 cm on the average, while the lead ice is taken to have a z_0 of 0.0001 to 0.001 m, with corresponding roughness elements of 3 mm to 3 cm. Radiation boundary conditions are employed at both upstream and downstream boundaries.

One significant modification to the original model [*Kantha and Mellor*, 1989] is the inclusion of frazil ice. Because of the disparate rates of heat and salt transfers at the ice-ocean interface in the model, supercooling occurs in the water column. This supercooling can be eliminated by bringing the water column back to freezing conditions and converting the temperature deficit to equivalent frazil ice in the water column at each time step. The resulting frazil ice is assumed to immediately accrete at the underside of the ice. This is the same approach used by *Mellor and Kantha* [1989] and *Häkkinen and Mellor* [1992]. We find that the inclusion of frazil ice increases the ice growth rates considerably. For a recent study of frazil ice formation in the laboratory the reader is referred to *Ushio and Wakatsuchi* [1993].

Finally, a major advantage of the current approach, compared with the scaling approaches to mixing parameterization based on similarity considerations, such as that presented by *Morison et al.* [1992], is the explicit calculation of turbulence fields.

5. Discussion of Results

We describe four sets of simulations. The first three simulate leads corresponding to advective cases of *Kozo* [1983] and *Morison et al.* [1992] and to *Smith and Morison*'s [1993] convective and advective cases. The model parameters in each case are chosen to reproduce the conditions of the original simulation as closely as possible. For example, no frazil ice formation is allowed, and ice salinity is taken to be a constant. The objective is to find out what improvements, if any, result from the refinements in the approach, especially from explicit turbulence parameterization and coupling of the ice and ocean.

The fourth set describes an attempt to simulate the two leads observed well during LEADEX [*LEADEX Group*, 1993] based on the observational data publicly available at present in the form of a LEADEX workbook. Here, however, we do account for frazil ice formation in the supercooled water column and the decrease of lead ice salinity with time. Even though this may seem contrary to observations, which showed little frazil ice formation, the conditions during LEADEX were anomalously warm and solar insolation nonnegligible, and wintertime Arctic leads are to be expected to generate significant amount of frazil ice.

5.1. *Kozo* [1983] Lead

Here we simulate *Kozo*'s [1983] fourth case with advection of 5 cm s^{-1} perpendicular to the axis of the lead. The lead width is 120 m, and the domain extends 120 m on both sides of the lead. The horizontal and vertical resolutions (5 m) are similar to *Kozo*'s [1983], except that the horizontal grid size is the same inside and outside the lead. There are additional levels in the top 5 m for a better depiction of the surface layer. The roughness scale z_0 is the same as by Kozo, 0.01 m outside and 0.001 m inside the lead. The mixed layer has a depth of 35 m and is bounded below by a strong halocline. The salinity in the mixed layer is 31 psu, and the change across the halocline is 0.6 psu. The lead ice is assumed to have a salinity of 10 psu. The water column is assumed to be freezing.

The principal difference is that the salt flux is computed from the ice growth rate and is not held constant and tur-

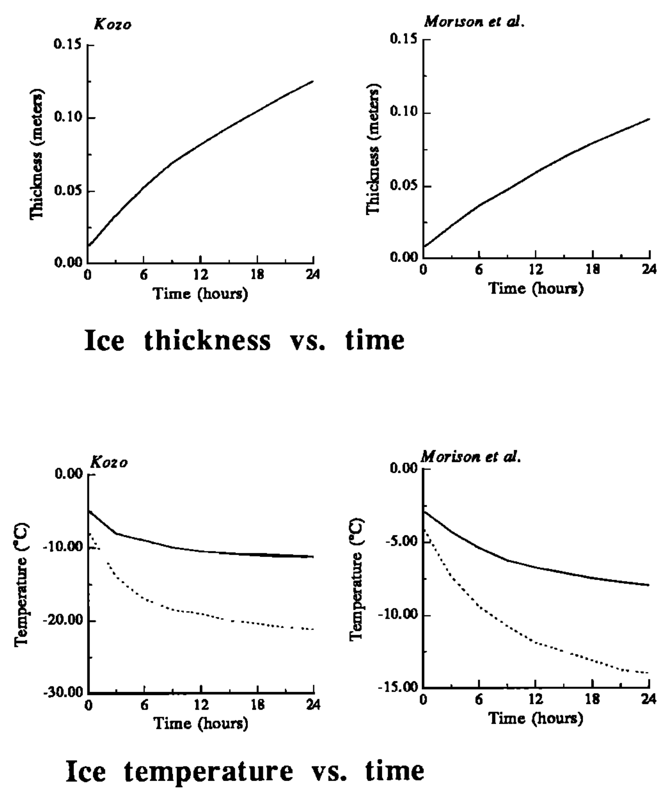

Figure 1. Ice thickness and temperatures as functions of time for *Kozo* [1993] and *Morison et al.* [1992] cases. The dotted line shows the ice surface temperature in the lead.

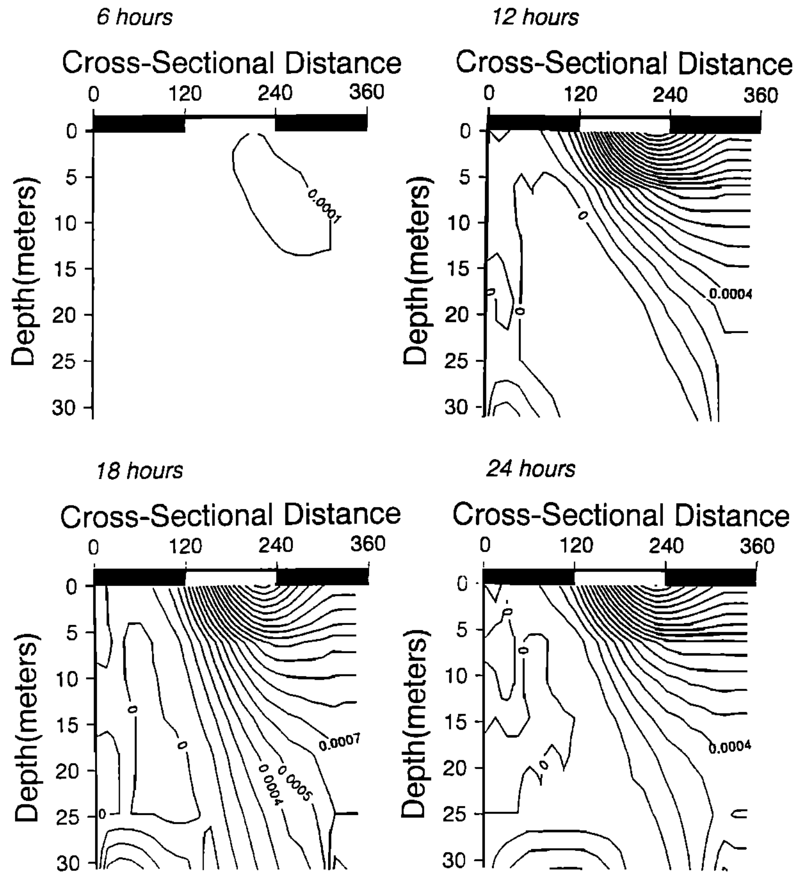

Figure 2. The salinity increase (in practical salinity units) above the initial mixed layer value at intervals of 6 hours, for *Kozo*'s [1983] advective case. The relative fluid motion is from left to right at 5 cm s^{-1}.

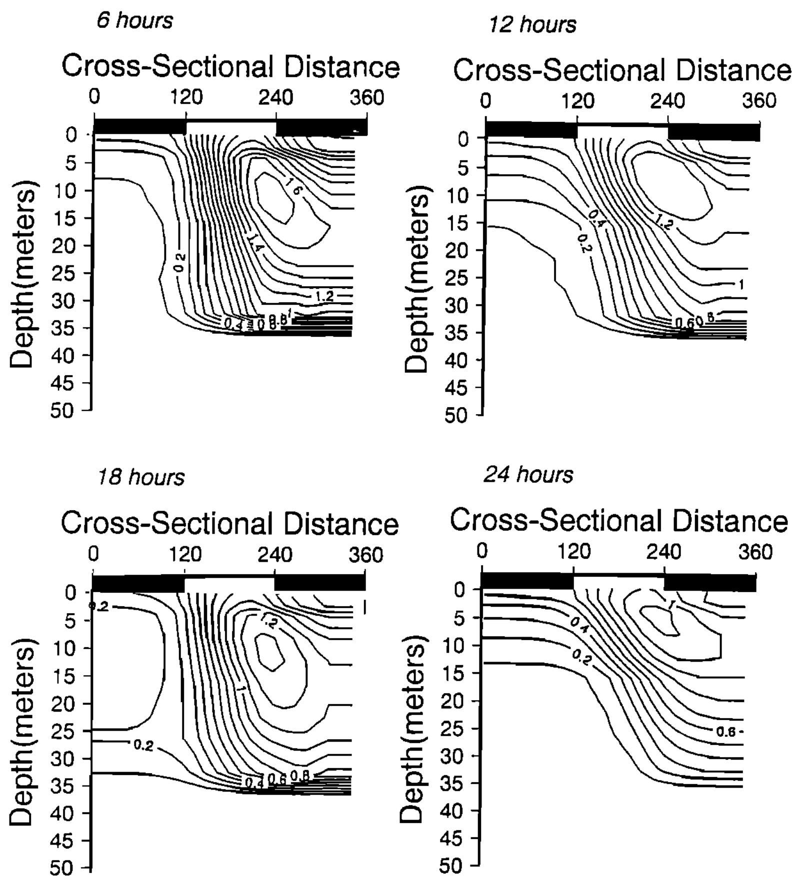

Figure 3. TKE (multiplied by 2) distribution in the lead for Kozo's advective case at intervals of 6 hr. The relative fluid motion is from left to right at 5 cm s^{-1}. Note the gradual decrease in the level of mixing below the lead.

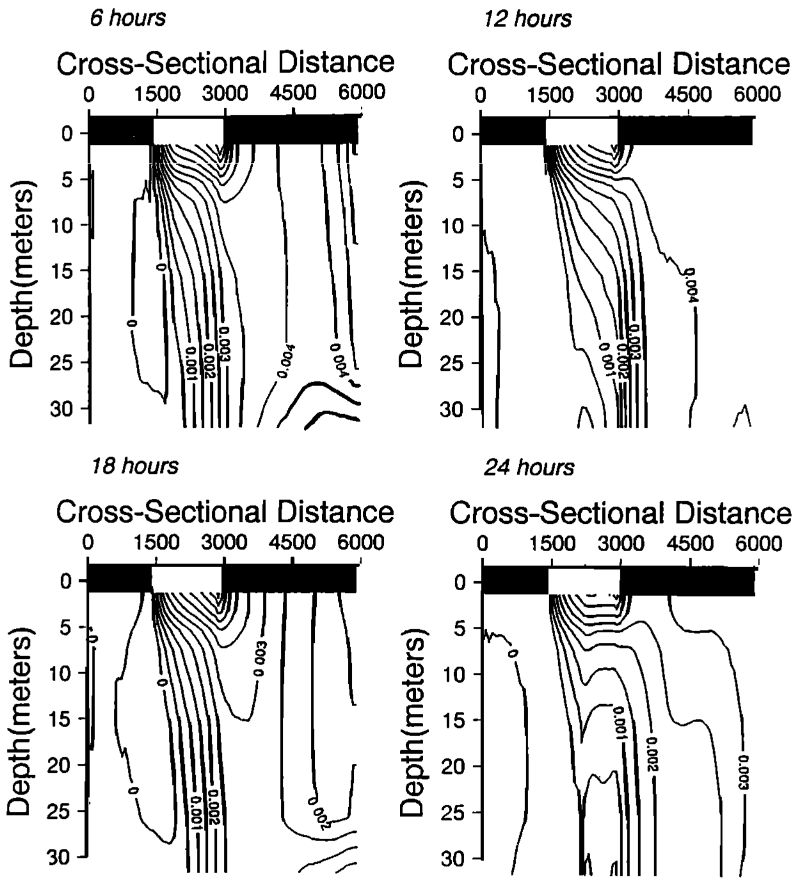

Figure 4. The salinity increase (in practical salinity units) above the initial mixed layer value at intervals of 6 hours, for *Morison et al.* [1992] lead. The relative fluid motion is from left to right at 20 cm s^{-1}.

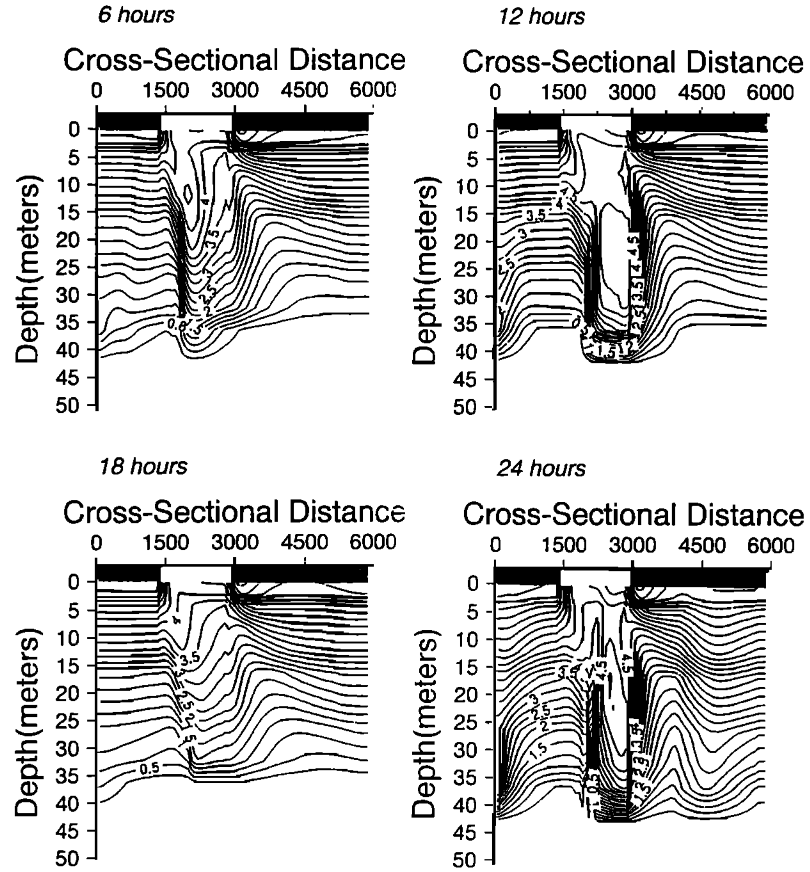

Figure 5. TKE (multiplied by 2) distribution in the lead for *Morison et al.* [1992] lead at intervals of 6 hours. The relative fluid motion is from left to right at 20 cm s^{-1}. Note the gradual decrease in the level of mixing below the lead. Note, also, the plumes at 12 and 24 hours.

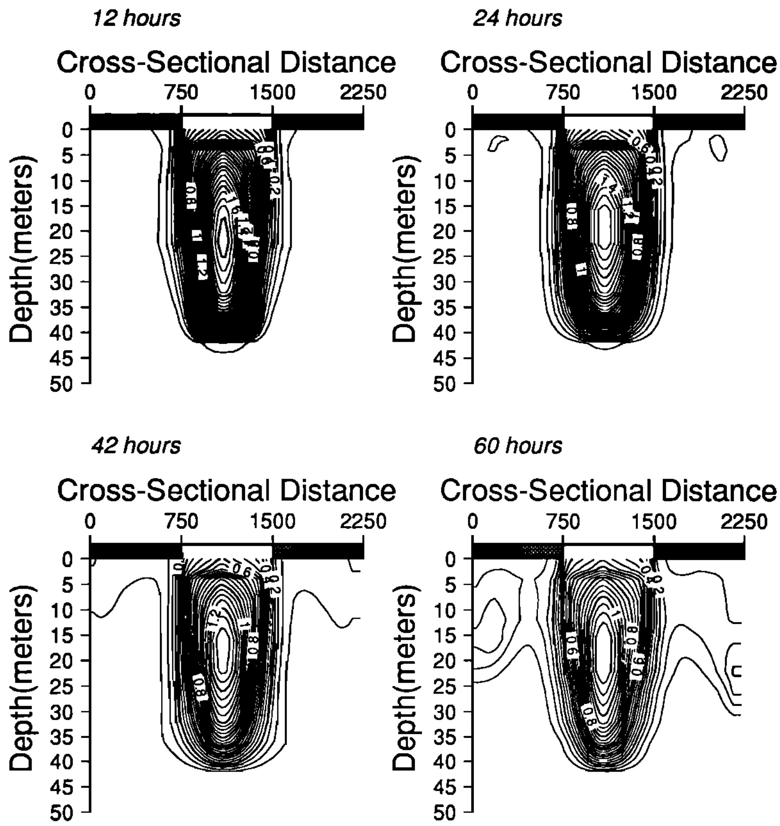

Figure 6. TKE distribution in the lead for *Smith and Morison* [1993] lead at 12, 24, 42, and 60 hours after the lead opening. Ice drift velocity is zero.

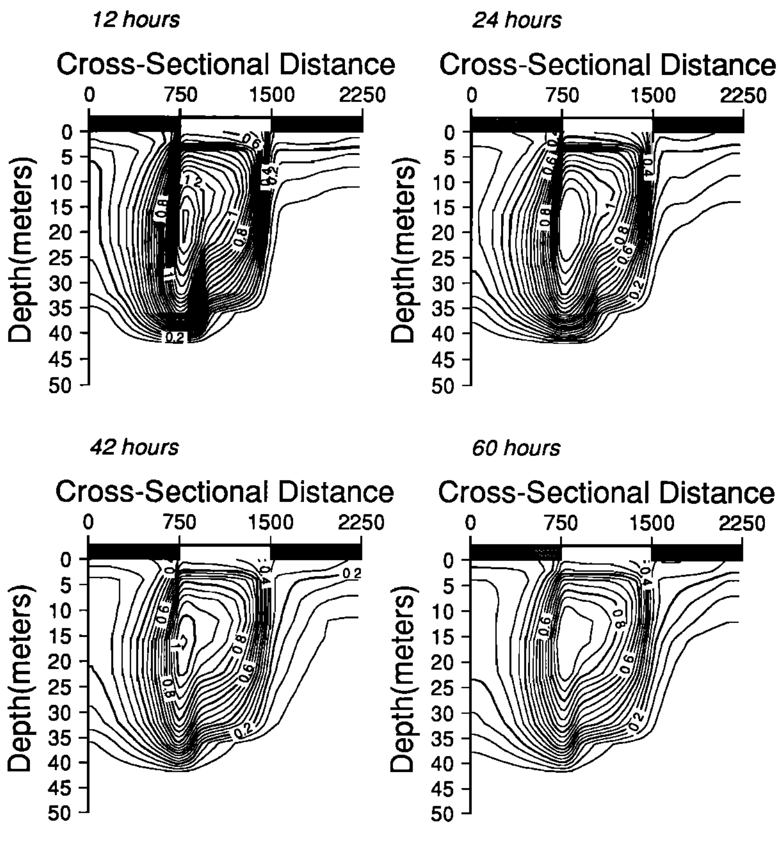

Figure 7. TKE distribution in the lead for *Smith and Morison* [1993] lead at 12, 24, 42, and 60 hours after the lead opening. Relative fluid motion is from right to left at 5 cm s^{-1}.

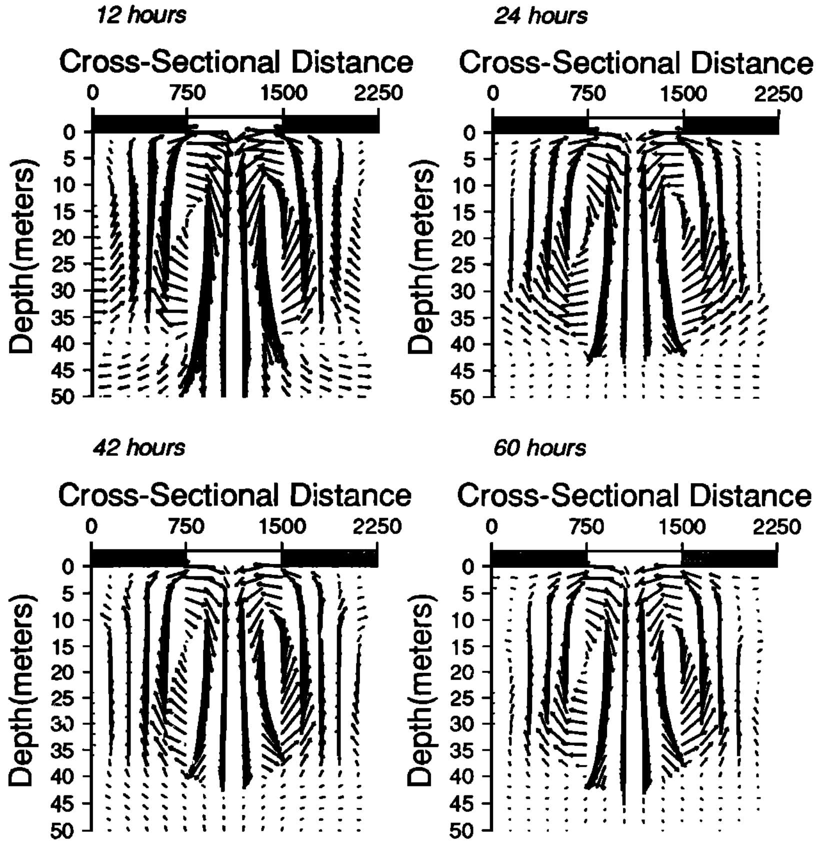

Figure 8. Velocity distribution in the lead for *Smith and Morison* [1993] lead at 12, 24, 42, and 60 hours after the lead opening. Ice drift velocity is zero. Note the deep impinging plume at the lead center and convective rolls at the ice edges.

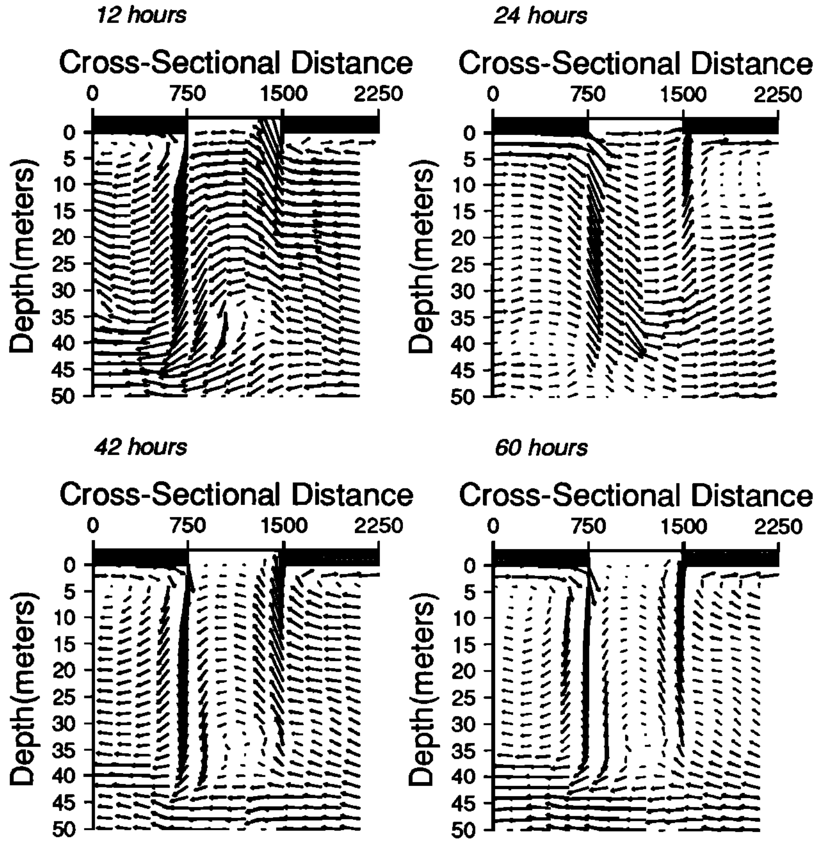

Figure 9. Velocity distribution in the lead for *Smith and Morison* [1993] lead at 12, 24, 42, and 60 hours after the lead opening. Relative fluid motion is from right to left at 5 cm s^{-1}. Note the inertial oscillation as indicated by plots at 24 hours and 42 hours.

bulence is explicitly computed. *Kozo* [1983] chose an ice growth rate of 1.25 cm h^{-1}, equivalent to a heat loss of 1200 W m^{-2}. Since the heat loss in the model is determined by the net heat balance at the air-ice interface and not just by the sensible heat flux, we chose, instead, to prescribe an air speed of 20 m s^{-1} and an air temperature of -25°C. Since the heat transfer coefficient is chosen to be 0.002 and the ocean temperature is -1.5°C, this corresponds to an initial sensible heat loss of about 1200 W m^{-2}. Nevertheless, in the model, ice builds up and the temperature at the air-ice interface decreases, leading to decreased sensible heat loss and lower ice growth. About 12 cm of ice accumulates at the end of a day.

Figure 1 shows the lead ice thickness and ice temperatures as functions of time for both *Kozo* [1983] and *Morison et al.* [1992] leads (see section 5.2). The ice growth rate decrease with time is consistent with what is known from observations of real leads. Since the salt flux is proportional to the rate of ice growth, it is clear that it should also decrease with time. Figure 2 shows the salinity increase above the initial mixed layer value at intervals of 6 hours (flow is from left to right due to ice drift). The maximum increase occurs at the trailing edge of the lead, and its magnitude is about 0.003 psu, decreasing gradually to 0.002 psu at the end of the day. Figure 3 shows the corresponding turbulence kinetic energy (TKE) distribution. The predominance of free convection immediately below the lead is evident in these plots. The maximum turbulence levels occur in the body of the mixed layer, slightly downstream of the trailing edge. The turbulence levels beneath and downstream of the lead are considerably elevated compared with those upstream. There is no evidence of episodic plume shedding at the downstream lead edge.

Overall, these simulations are in good agreement with *Kozo*'s [1983]. Clearly, the salinity distribution shows evidence of lead activity, and so does the turbulence intensity. The salinity perturbation is qualitatively similar to that of *Morison et al.*'s [1992] simulations, which are discussed next.

5.2 *Morison et al.* [1992] Lead

Here we simulate a 1400-m-wide lead with an advection velocity of 20 cm s^{-1}. The mixed layer depth is 40 m, and its salinity is 32 psu. The mixed layer water is assumed to be freezing. The roughness scales are the same as in the above simulation. There is a strong halocline at the base of the mixed layer. The air temperature is -20°C, and the wind speed is 10 m s^{-1}. These conditions lead to an initial ice growth rate of 0.625 cm h^{-1}, the same as that assumed by *Morison et al.* [1992], but the ice growth decreases with time and about 9.5 cm of ice accumulates by the end of the day. Figure 1 shows the ice thickness and ice temperatures as functions of time.

Figure 4 shows the salinity perturbation, which is qualitatively consistent with that of *Morison et al.* [1992], with the maximum perturbation appearing at the trailing edge (the flow is from left to right due to ice drift). However, the magnitudes are much smaller, about 0.005 to 0.007 psu, compared with 0.018 in *Morison et al.*'s [1992] case. We believe that the increased mixing levels are responsible for weaker unstable stratifications observed in this model. Figure 5 shows the TKE distributions. The maximum occurs near the trailing edge of the lead. Even though the shear generation is quite strong away from the lead, the turbulence levels in the body of the mixed layer underneath the lead are elevated well above the values upstream and downstream. Shedding of a salt plume at the downstream edge of the lead is evident in the TKE plots at 12 and 24 hours from the time of lead opening. The velocity fields (not shown), once again, exhibit vigorous inertial oscillations, especially below the mixed layer.

Unlike the original study the present results are dynamically consistent. They also have the additional advantage of the convection driven by the salt flux being coupled to ice growth, as well as that of second-moment closure of turbulent mixing. It is also significant that episodic shedding occurs during this simulation.

5.3. *Smith and Morison* [1993] Lead

These simulations attempt to discern any differences in simulations of *Smith and Morison* [1993] due to improved mixing and coupling to ice growth. The lead width is 750 m, and the mixed layer depth is taken to be 40 m, with a strong halocline below. All other conditions are similar to the LEADEX lead 3 case described below. Figures 6 and 7 show TKE distributions under the lead for ice drifts of 0 and 5 cm s^{-1}, respectively (the flow is from right to left). Figures 8 and 9 show the corresponding velocity distributions. The results are qualitatively similar to other free convective and advective situations studied here (see LEADEX 3 simulations below, for example). The most notable difference with respect to the *Morison et al.* [1992] study is the absence of episodic plume shedding in both cases. While there is a plume at the trailing lead edge for the advective case, it does not appear to shed. We suspect that intense but realistic mixing levels in this model might be responsible, but further exploration of model parameter space is needed to delineate conditions for episodic plume shedding.

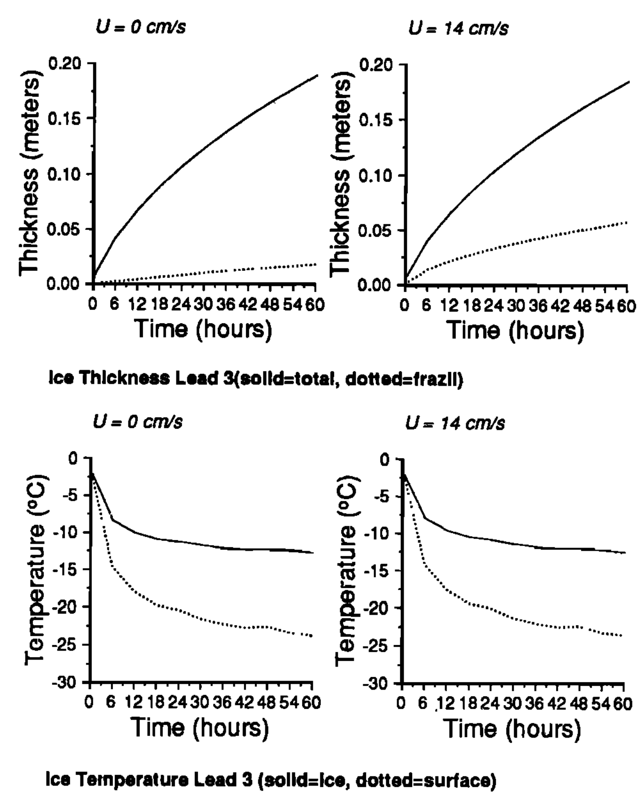

Figure 10. Ice thickness and temperatures as functions of time for lead 3. The dotted lines show frazil ice thickness and the ice surface temperature in the lead.

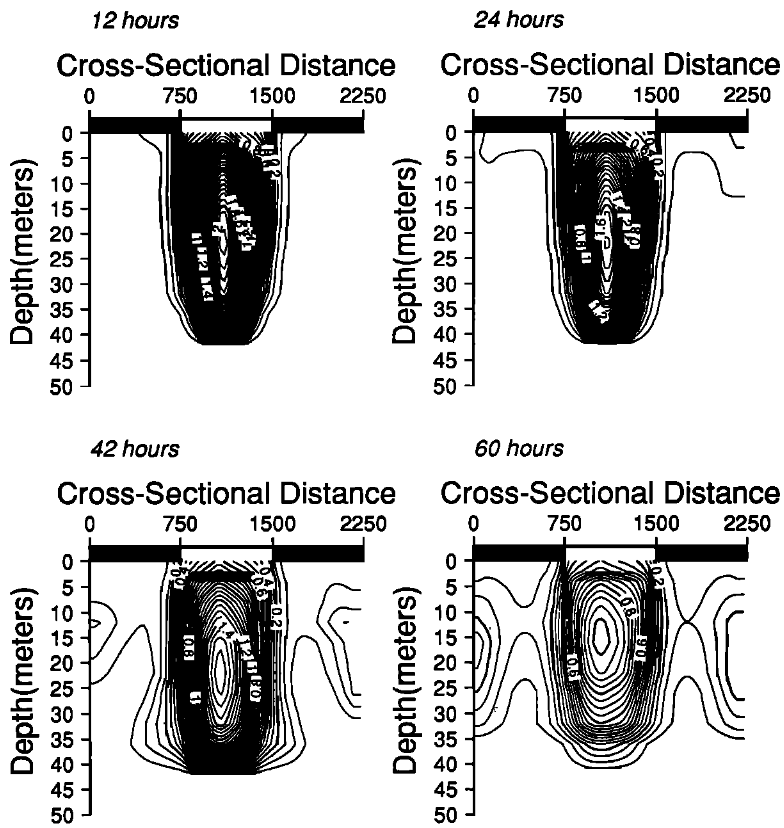

Figure 11. TKE distribution under lead 3 at 12, 24, 42, and 60 hours after the lead opening. for zero ice drift velocity. Note the gradual decrease of TKE with time.

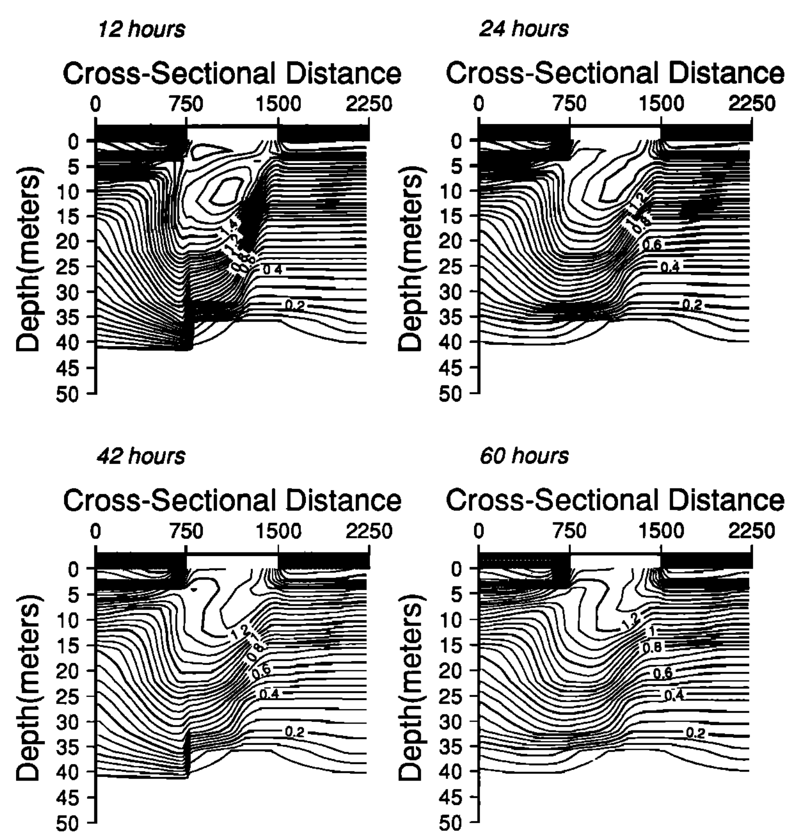

Figure 12. TKE distribution under lead 3 at 12, 24, 42, and 60 hours after the lead opening. Relative fluid motion is from right to left at 14 cm s^{-1}.

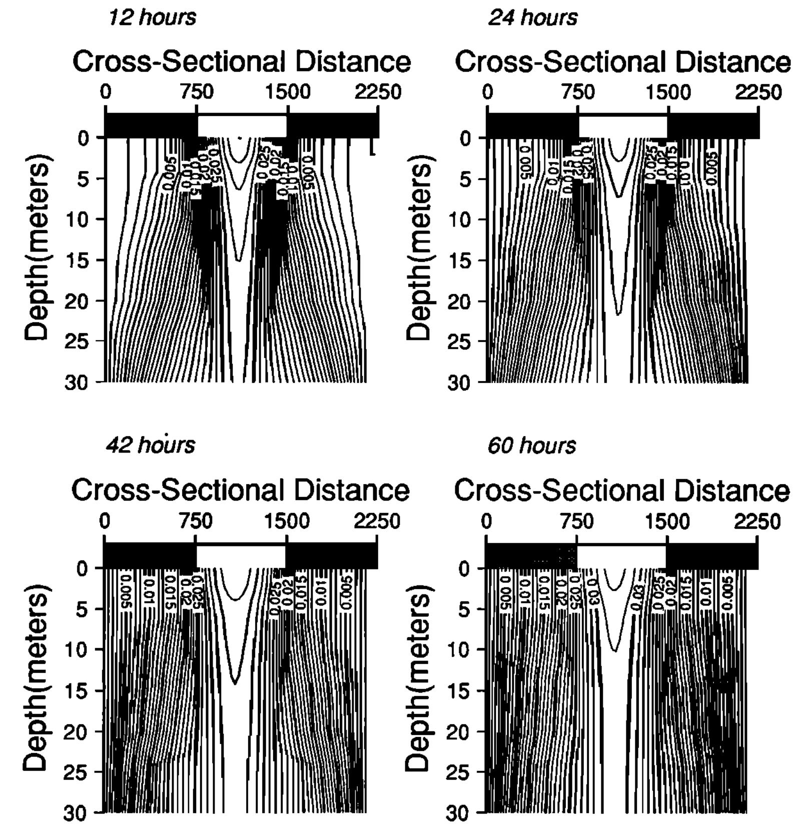

Figure 13. The salinity increase (in practical salinity units) above the initial mixed layer value for lead 3 at 12, 24, 42, and 60 hours after lead opening for zero ice drift.

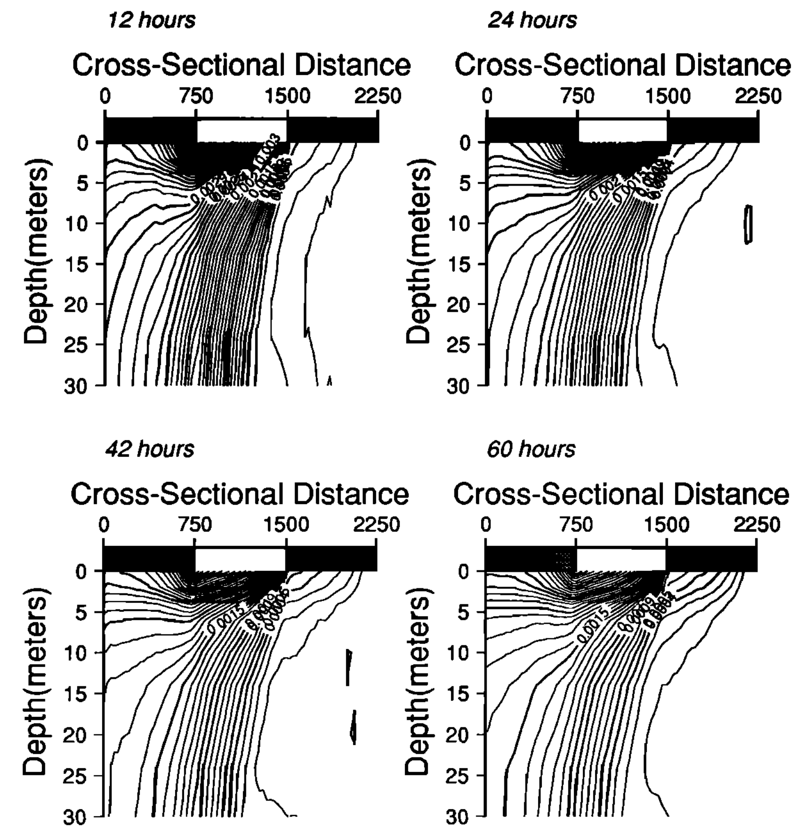

Figure 14. The salinity increase (in practical salinity units) above the initial mixed layer value for lead 3 at 12, 24, 42, and 60 hours after lead opening. The relative fluid motion is from left to right at 14 cm s^{-1}.

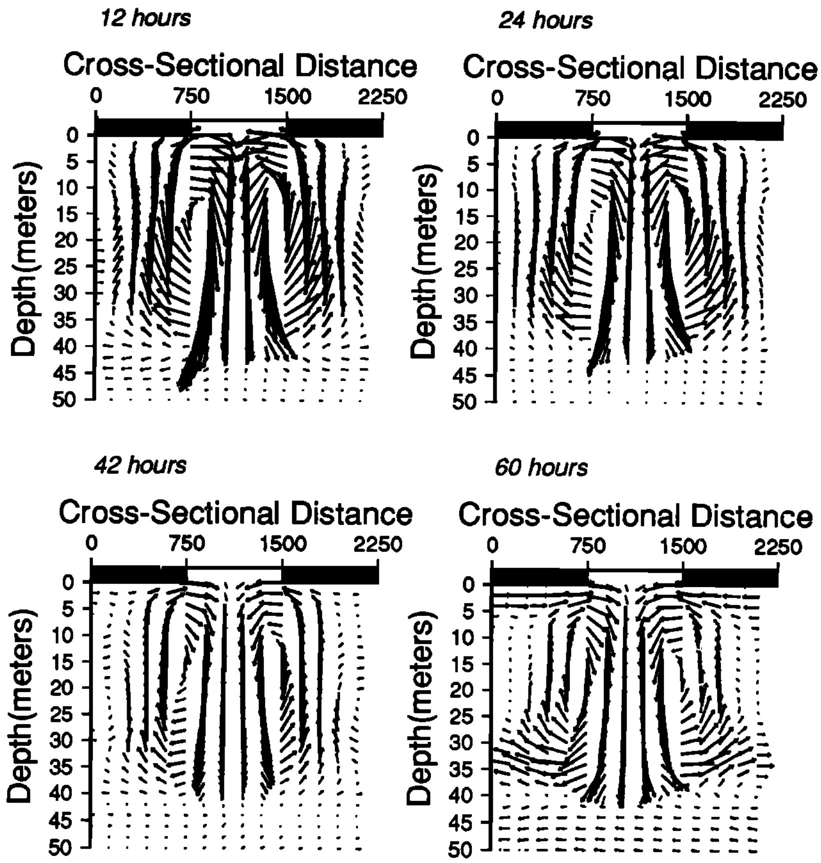

Figure 15. Velocity distribution under lead 3 at 12, 24, 42, and 60 hours after the lead opening for zero ice drift. Note the deep impinging plume at the lead center and convective rolls at the ice edges.

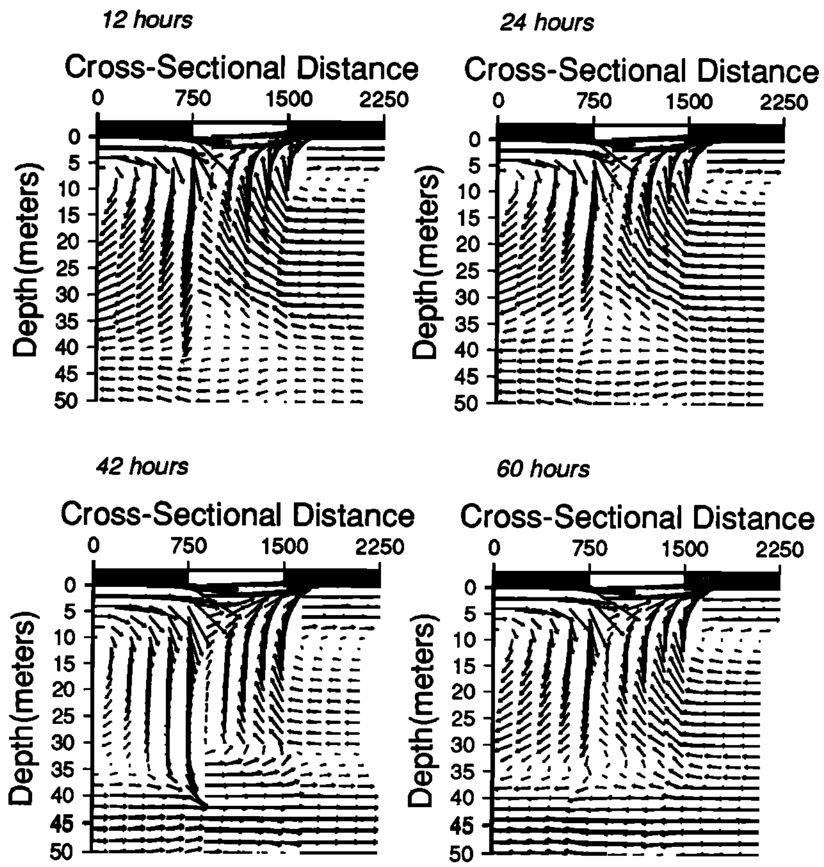

Figure 16. Velocity distribution under lead 3 at 12, 24, 42, and 60 hours after the lead opening. Relative fluid motion is from right to left at 14 cm s^{-1}. Note the inertial oscillation as indicated by plots at 24 hours and 42 hours.

5.4. LEADEX Leads

We next describe simulations of the leads observed during LEADEX. The LEADEX observation team was able to make detailed measurements of two leads, leads 3 and 4, (J.H. Morison et al., unpublished manuscript, 1994), with contrasting characteristics [*LEADEX Group*, 1993]. Lead 3 was about 500-1000 m wide, and the ice drift rate was quite high, about 0.14 m s^{-1}, while lead 4 was 130 m wide, and the ice velocity was low at about 0.04 m s^{-1}. Turbulent dissipation measurements suggest that forced convection may have been dominant at the former, although narrow convective plumes were observed. An inertially modulated jet was also observed near the mixed layer base. At lead 4 the convective plumes were concentrated near the edges of the lead.

The measured temperature and salinity structure underneath lead 3 are shown by *Muench et al.* [this issue]. The water in the mixed layer is at freezing conditions with a temperature of about -1.64°C and a salinity of about 30.1 psu. The mixed layer depth is roughly 30 m, and there is a strong increase in temperature at the base of the mixed layer of about 0.4°C. The conditions at lead 4 are roughly similar, with a temperature of -1.62°C and salinity of 29.9 psu. The mixed layer depth and the temperature change at its base are roughly the same as under lead 3. The similarity of the underlying mixed layer in the two leads is not surprising, since they were found within a few days of each other and only 30 km apart. We therefore assume the model mixed layer to have initially similar properties for both these leads; the mixed layer depth of 30 m, temperature of -1.63°C and salinity of 30.0 psu. The profile below the mixed layer is also assumed to be the same, as indicated by observations.

There is some uncertainty as to the width of lead 3. It is quoted as being 500 to 1000 m wide. We take its width to be 750 m in the model. The width of lead 4 is taken to be 130 m. The horizontal grid size for the former is 30 m, while it is 15 m for the latter. The model domain extends a full lead width on both sides of the numerical lead. The depth of the water column is taken as 100 m, with no momentum or other fluxes at the bottom. The number of vertical levels is 25, with a grid spacing of 5 m below a depth of 10 m, but decreasing gradually to 0.5 m near the surface. The thickness of the first-year pack ice surrounding the leads has been observed to be close to 1 m, and this is taken as the depth of ice surrounding the model leads.

The horizontal resolution in the model is chosen to be consistent with the simulations reported earlier. This resolution is not fine enough to resolve the spatial structure of convection underneath the leads, especially the narrow, plumelike features typical of convection, whether under a lead or above a heated surface. LEADEX observations indicate spatial scales of a few tens of meters in lead 3 and very narrow plumes. A much higher resolution would be necessary to simulate these aspects of LEADEX leads. What we attempt to depict here is more akin to a long-term average of the circulation in a refreezing lead.

Model simulations are started by slowly ramping up external forcing over a period of 0.5 days, roughly an inertial period at these latitudes. The lead is kept closed until then and then suddenly opened up at the end of 0.5 days. Integration is continued to 3.0 days. The results are shown at 12, 24, 42, and 60 hours from opening of the leads. The model computes the full thermodynamic balance at the ice-atmosphere interface, including the values of the short-wave and long-wave solar radiation incident on the ice, the sensible and latent fluxes, as well as the back radiation [*Kantha and Mellor*, 1989; *Mellor and Kantha*, 1989]. The air temperature is fairly well known (roughly -26°C for lead 3 and -29°C for lead 4), but details about the prevailing winds and detailed heat balance estimates are not yet available. We adjusted the meteorological parameters to obtain an initial (iceless) net heat loss rate corresponding to the observed initial ice growth rate and kept them unchanged during the model simulation. It is our objective to approximate the observed leads as closely as possible in the numerical model for purposes of clarifying the physical processes involved and not necessarily to duplicate the conditions exactly.

The lead ice is much smoother than the surrounding ice, in general, in the absence of rafting. The roughness scale z_0 is therefore taken as 0.01 m around the lead but 0.0001 m in the lead itself (results for z_0 value of 0.001 m in the lead are not much different). The resulting drag reduction in the lead is quite important to the lead-driven mixing and circulation in the mixed layer below. This distinction is also important to the ice growth, since as *Mellor and Kantha* [1989] and *McPhee* [1992] have shown, the heat and mass transfer in a boundary layer on a rough wall has some salient features that can not be ignored. Specifically, the heat and mass transfers are functions of molecular diffusivities of the fluid, even when the flow is turbulent [*Yaglom and Kader*, 1974].

An important finding during LEADEX was the apparent lack of influence of the short-wave solar radiation absorbed by the water column under the lead on the salt-driven convection in the mixed layer, which is not surprising, since temperature fluctuations around freezing do not greatly influence the density fluctuations [*LEADEX Group*, 1993]. We therefore ignore penetrative solar heating of the lead ice and the water

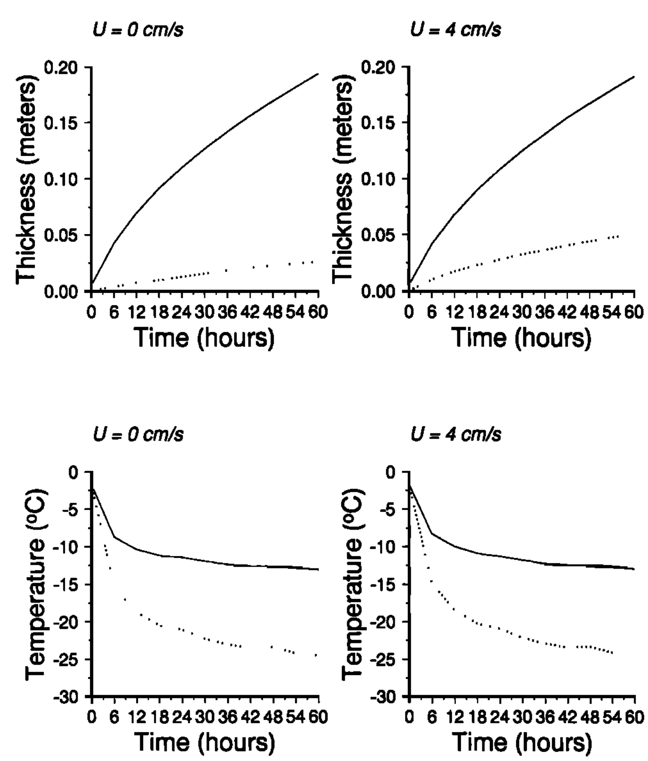

Figure 17. Ice thickness and temperatures as functions of time for lead 4. The dotted lines show frazil ice thickness and the ice surface temperature in the lead.

below and assume that all the solar radiation is absorbed at the ice surface. This ignores the small diurnal modulation of the ice growth and the modulation in ice temperature, observed during LEADEX, due to absorption of solar radiation in the water column underneath the thin lead ice during the day [*LEADEX Group*, 1993]. Another significant finding from LEADEX was the formation of frost flowers on the thin ice in the lead, leading to increased albedo and a decrease in the solar radiation absorbed. We account for this by taking the surface albedo of the ice cover to correspond to that of snow rather than ice.

LEADEX observations showed that the salinity in the lead ice was initially very high (20-25 psu) but decreased to more normal values of 10-15 psu as the ice thickened. Therefore the salt flux driving convection below tends to have a peaked form, with lower values during the initial and final stages of a lead's lifetime. We made an empirical fit to the LEADEX observations by assuming the ice salinity to be a function of the ice thickness of the following form:

$$S_i = 18\left(1 - \frac{t_i}{0.22}\right)^{0.75} + (S_w - 18) \qquad t_i < 0.22$$
$$S_i = 12 \qquad t_i \geq 0.22 \qquad (13)$$

where S_i is ice salinity (in practical salinity units) and t_i is the ice thickness (in meters). The use of this empirical fit in the model enables the corresponding salt flux to increase to a peak due to initially larger ice growth rates, but smaller salt extrusion, and then decrease gradually due to decreasing ice growth rates.

We have performed two simulations for each model case, one with the observed ice drift speeds and the other with zero ice drift to simulate free convective conditions. Figure 10 shows ice thickness as a function of time for the wide lead 3 observed during the April 6 to April 9 time period. The ice grows to about 12 cm thickness during the first 24 hours, in rough accordance with LEADEX observations (two independent measurements indicated values of 14 cm and 10 cm ice growth during the first 24 hours and the average value is 12 cm), but the growth rate decreases due to the insulating effect of lead ice, leading to a thickness of about 18 cm at the end of 60 hours. There is little change in the ice growth rates due to advection, although the frazil ice contribution increases twofold owing to the availability of advected water masses at freezing conditions that can be supercooled more efficiently, leading to higher frazil ice production. Since the net heat loss from the lead remains roughly the same, the net ice growth rate also remains approximately same.

Figure 10 also shows the ice and ice surface temperatures as a function of time; a slight diurnal modulation of the ice surface temperature can be seen in both cases. The turbulence fields in the mixed layer underneath (Figures 11 and 12) show marked differences. For the stationary lead case (Figure 11), turbulence is confined to the immediate vicinity of the lead itself, with initial values of TKE exceeding 2 cm^2 s^{-2} but decreasing gradually to peak values of less than 1 cm^2 s^{-2} at the end of 60 hours. The half- life time appears to be about 2 days. The turbulence field is markedly different for the advective case, which corresponds to the observed situation for lead 3. The high advection velocity leads to strong shear generation of turbulence both upstream and downstream of the lead in the surrounding rough ice. While the convection driven by salt extrusion is clearly evident at the end of 12 hours, its signature is weak at the end of 60 hours. In marked contrast to the zero-drift case, there is vigorous turbulence both upstream and downstream of the lead, which would make it difficult to detect an active lead by the level of turbulence underneath.

Figures 13 and 14 show the increase in salinity (over the initial value in the mixed layer) for the free convective and the advective situations. The salinity increase is an order of magnitude larger in the former case (peak values around 0.03 psu compared with 0.003 psu in the latter), while markedly asymmetric in the latter. The peak value in salinity increase is also confined to the vicinity of the near-surface of the lead itself when advection is present, whereas the increase is more uniformly distributed over the mixed layer for the free convective case.

Figures 15 and 16 show the circulation underneath the lead (note that the vertical velocities are magnified 50 times). The circulation is quite symmetric for zero ice drift, with convective rolls at the ice edges, as can be seen in Figure 15. A strong inward jet is clearly evident at 60 hours, with a corresponding outward flow at the base of the mixed layer. Inertial oscillations are also evident, especially below the mixed layer. The circulation under a drifting lead is markedly different, as seen in Figure 16. The vertical velocity is directed toward the surface at the upstream ice edge (ice is moving from left to right) but downward at the downstream edge. Vigorous inertial oscillations are seen under the mixed layer. However, we did not see any evidence of episodic plume shedding at the lead edges either for the stationary or drifting cases.

Figure 17 shows the ice thicknesses and ice temperatures for the narrow lead 4 for ice drift velocities of 0 and 4 cm s^{-1}. Not surprisingly, the growth rates are comparable with that of lead 3, since the meteorological and mixed layer conditions were roughly similar. Figures 18 and 19 show the corresponding turbulence velocity fields. Ice motion concentrates TKE at the downstream edge of the lead, whereas for a stationary lead the TKE field is symmetric with a maximum at the center of the lead. Also, the maximum occurs closer to the ice undersurface. Because of the small drift velocity, convective activity underneath the lead is clearly discernible, even after 60 hours. Once again, there was no evidence of episodic plume shedding for lead 4 in either case. Figure 20 shows the velocity field for the advective case. Plots at 24 and 42 hours (inertial period at this latitude is roughly 12 hours) clearly show vigorous inertial currents in the water column.

6. Concluding Remarks

We have presented a numerical model of the coupled ice-ocean system that provides a quantitative description of a refreezing lead, especially the evolution of the ice cover and the mixed layer below. The results indicate that a strong convection driven by the extruded brine in a refreezing lead drives vigorous mixing in the mixed layer immediately below, irrespective of the advective velocity of ice. Turbulence intensities reach quite high values during the initial phases of refreezing but weaken gradually with a half-life time of about 2 days. Inertial oscillations are superimposed on the resulting currents and are especially vigorous below the mixed layer. The rate of ice buildup is nearly independent of the ice drift velocity but is a strong function of the heat loss rate at the

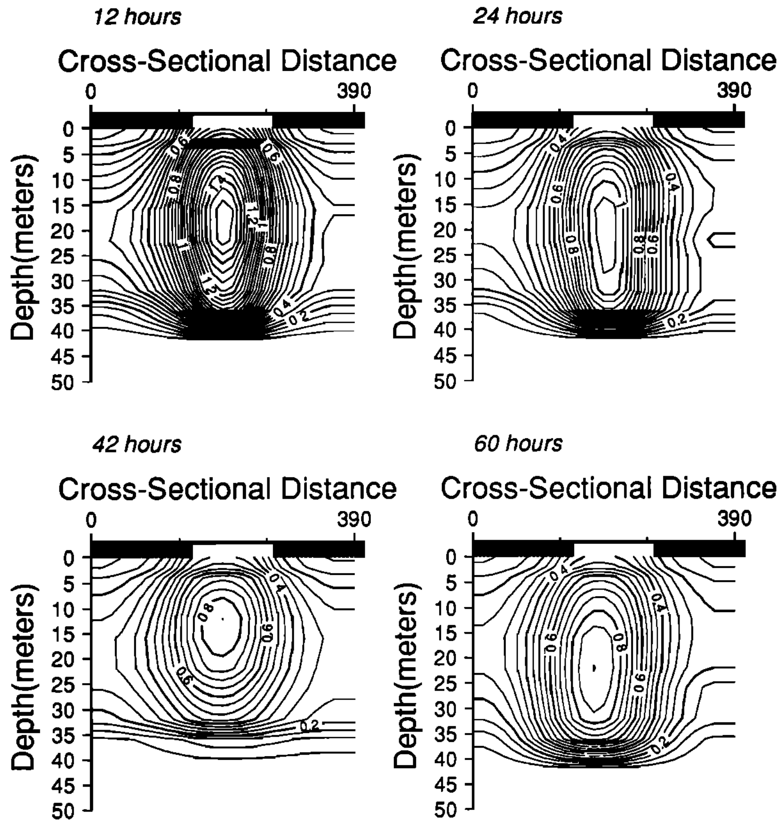

Figure 18. TKE distribution under lead 4 at 12, 24, 42, and 60 hours after the lead opening for zero ice drift velocity. Note the gradual decrease of TKE with time.

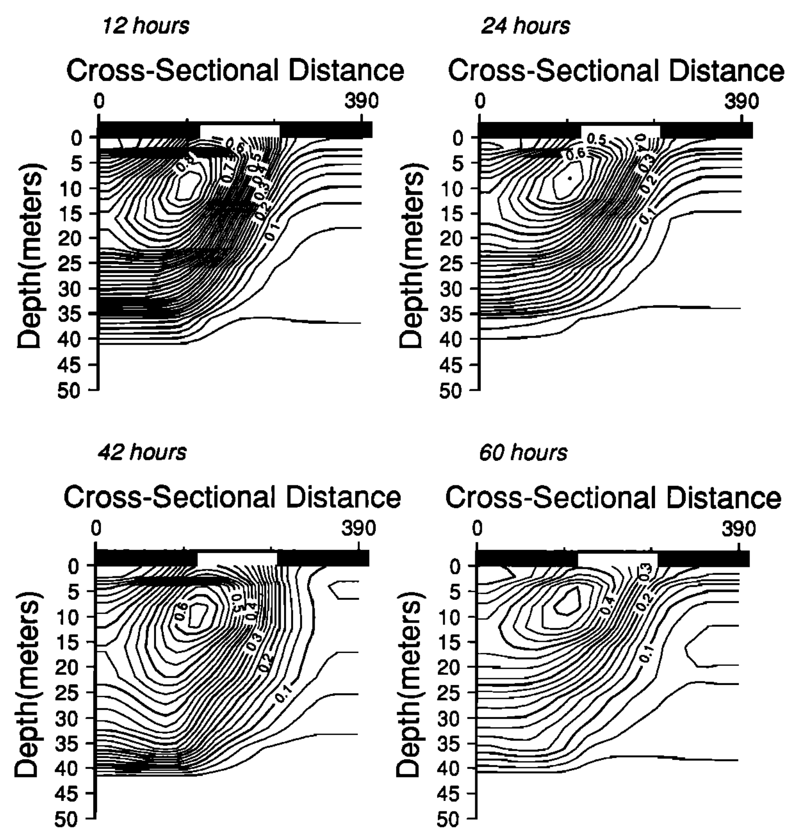

Figure 19. TKE distribution under lead 4 at 12, 24, 42, and 60 hours after the lead opening. Relative fluid motion is from right to left at 5 cm s^{-1}.

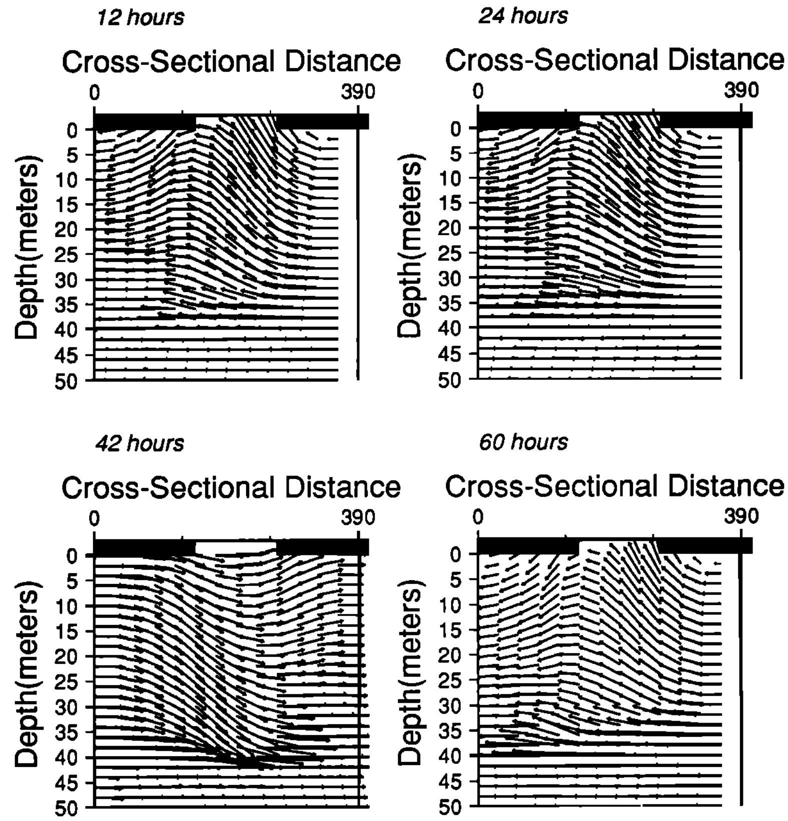

Figure 20. Velocity distribution under lead 4 at 12, 24, 42, and 60 hours after the lead opening. Relative fluid motion is from right to left at 5 cm s^{-1}. Note the inertial oscillation as indicated by plots at 24 hours and 42 hours.

surface. In model simulations of LEADEX leads the ice builds up to a thickness of over 12 cm in the first 24 hours in a refreezing lead, in accordance with observations, with a significant contribution coming from frazil ice formation in the supercooled water below. Not surprisingly, since the water below is at or close to freezing, advection of water masses past the lead due to ice motion or prevailing currents does not alter the refreezing rate substantially, even though the frazil ice contribution shows a significant increase.

Advection does affect the local properties in the mixed layer immediately below and downstream of the lead. For example, the increase in salinity, an indicator of the intensity of the refreezing process in a lead, depends very much on the motion of ice cover relative to the underlying water. For large advective velocities the salinity increase is an order of magnitude smaller than the purely convective situation and the turbulence is dominated by that generated by shear underneath the rough ice upstream of the lead, which tends to mask that generated by convection in the lead itself. Inertial motions are evident, especially below the mixed layer. This is to be expected in any rotating fluid under time-dependent forcing. Convective cell is confined to the downstream edge of the lead in agreement with the simulations of *Smith and Morison* [1993]. For a stationary lead, refreezing gives rise to an inward jet underneath the ice and outward flow at the base of the mixed layer. Vertical motion is in the form of convective cells centered at the lead edges.

However, contrary to *Smith and Morison* [1993] simulations, no clear evidence of strong episodic eddy shedding exists in the current simulations of LEADEX leads. We did observe evidence for shedding of plumes for the case considered by *Morison et al.* [1992]; it is possible that high drift speeds and broad leads might be more conducive to episodic plume shedding in the current model. The intense turbulence induced by convection might play an important role in episodic shedding and spatial structure. It is possible that a higher horizontal resolution might be essential to resolving the spatial structure and simulating episodic shedding, especially in view of the intense mixing levels, a situation Morison et al. circumvented by choosing not to parameterize convective mixing in their model. It is not clear how the parameterization of mixing would affect the sensitive process of plume shedding at a lead edge; further studies are needed to delineate the conditions for plume shedding.

While this study has made further progress in modeling Arctic leads, it is clear that more needs to be done. One salient aspect of all lead simulations is that the salt flux is assumed to be proportional to the ice growth rate and uniform across the lead. There is observational evidence to indicate that the salt rejection from the lead ice might be more episodic and nonuniformly distributed across the lead. With some guidance from LEADEX observations, it might be possible to account for the episodic salt rejection by using an artificial reservoir of salt that is emptied into the ocean at predetermined intervals. This is akin to simulating melt ponds on the ice surface during the melting season [*Mellor and Kantha*, 1989].

The ice distribution in a lead is often nonuniform. The lead ice is initially in the form of frazil ice, and as accretion takes place, ice is blown to the leeward side of the lead, keeping the upstream side ice free. This situation could lead to larger ice production rates than the model simulations indicate. In lead models, once ice begins to form, it completely covers the lead surface and tends to attenuate the heat loss, whereas in a real lead the freezing water is kept exposed to the air on the upstream side, until sufficient ice thickness builds up. The ice formation is therefore likely to be a stronger function of the wind speed in the lead, since under calm conditions there is a tendency to form continuous ice cover. This effect needs to be suitably parameterized.

For winter leads, frazil ice formation in the lead is inevitable. However, during early spring, penetrative solar heating in the water column tends to suppress frazil ice formation, at least during the day. This is apparently the situation observed during LEADEX. Appropriate modifications to allow penetrative heating under ice are also needed.

In this study we have not attempted to duplicate the observed lead situation exactly. For example, the spatial structure observed underneath the leads is not simulated. It would be interesting to see if the spatial structure can be depicted by increased horizontal resolution. When that is accomplished, there is a need for detailed comparisons with data from LEADEX observations, including those on turbulence, water mass properties, and currents in and around a refreezing lead.

Although the feedback between the ABL over the lead and the oceanic mixed layer (OML) underneath cannot be large, it would be instructive to couple a simple ABL model to the ice-ocean coupled lead model to simulate the effects of changing roughness and heat transfer coefficients on the ABL and the OML.

Acknowledgments. Owing to a combination of circumstances, this study could not be supported by the LEADEX program. We thank Tom Curtin of the Office of Naval Research for his continued encouragement and interest in this study and bearing the publication expenses. A very small fraction of L. H. K.'s support during this study came from the NOMP program of the Office of Naval Research administered by Bob Peloquin, under contract N00014-92J-1572. Thanks also go to Jamie Morison for providing the LEADEX "workbook" just in time to enable the completion of this study. Comments from an anonymous reviewer helped catch an embarrassing transcription error in the solution of equation (6), and we thank him and a second reviewer for their thorough and constructive reviews. Todd Arbetter's help in plotting and model running is also acknowledged.

References

Anderson, D. L., Growth rate of sea ice, *J. Glaciol.*, *3*, 1170-1172, 1961.

Barry, R. G., M. C. Serreze, J. A. Maslanik, and R. H. Preller, The Arctic sea ice-climate system: Observations and modeling, *Rev. Geophys.*, *31*, 397-422, 1993.

Deardorff, J. W., Progress in understanding entrainment at the top of the mixed layer, in *Workshop on the Planetary Boundary Layer*, edited by J. C. Wyngaard, pp. 36-66, American Meteorological Society, Boston, Mass., 1980.

Doyle, J. D., and T. W. Warner, Mesoscale coastal processes during GALE IOP 2, *Mon. Weather Rev.*, *118*, 283-308, 1990.

Galperin, B., L. H. Kantha, S. Hassid, and A. Rosati, A quasi-equilibrium turbulent energy model for geophysical flows, *J. Atmos. Sci.*, *45*, 55-62, 1988.

Glendening, J. W., and S. D. Burke, Turbulent transfer from an Arctic lead: A large eddy simulation, *Boundary Layer Meteorol.*, *59*, 315-339, 1992.

Hadlock, R., and C. W. Kreitzberg, The experiment on rapidly intensifying cyclones over the Atlantic (ERICA) field study: Objectives and plans, *Bull. Am. Meteorol. Soc.*, *69*, 1309-1320, 1988.

Häkkinen, S., and G. L. Mellor, Modeling the seasonal variability of a coupled arctic ice-ocean system, *J. Geophys. Res.*, *97*, 20,285-20,304, 1992.

Häkkinen, S., G. L. Mellor, and L. H. Kantha, Modeling deep convection in the Greenland Sea, *J. Geophys. Res.*, *97*, 5389-5408, 1992.

Kantha, L. H., and C. A. Clayson, An improved mixed layer model for geophysical applications, *J. Geophys. Res.*, in press, 1994.

Kantha, L. H., and G. L. Mellor, A two-dimensional coupled ice-ocean model of the Bering Sea marginal ice zone, *J. Geophys. Res.*, *94*, 10,924-10,936, 1989.

Kozo, T. L., Initial model results for arctic mixed layer circulation under a refreezing lead, *J. Geophys. Res.*, *88*, 2926-2934, 1983.

LEADEX Group, The LEADEX Experiment. *Eos Trans. AGU*, *74*, 393-397, 1993.

Maykut, G. A., Energy exchange over young sea ice in the central Arctic, *J. Geophys. Res.*, *83*, 3646-3658, 1978.

McPhee, M. G., A time-dependent model for turbulent transfer in a stratified ocean boundary layer, *J. Geophys. Res.*, *92*, 6977-6986, 1987.

McPhee, M. G., Turbulent heat flux in the upper ocean under sea ice, *J. Geophys. Res.*, *97*, 5365-5380, 1992.

Mellor, G. L., and L. H. Kantha, An ice-ocean coupled model, *J. Geophys. Res.*, *94*, 10,937-10,954, 1989.

Mellor, G. L., and T. Yamada, Development of a turbulence closure for geophysical fluid problems, *Rev. Geophys.*, *20*, 851-875, 1982.

Moeng, C.-H., and P. P. Sullivan, Comparison of shear- and buoyancy-driven planetary boundary layer flows, *J. Atmos. Sci.*, *51*, 999-1022, 1994.

Morison, J . H., Forced internal waves in the Arctic ocean, Ph.D. thesis, Dep. of Geophys., Univ. of Wash., Seattle., 1980.

Morison, J. H., M. G. McPhee, T. B. Curtin, and C. A. Paulson, The oceanography of winter leads, *J. Geophys. Res.*, *97*, 11,199-11,218, 1992.

Muench, R. D., K. Jezek, and L. H. Kantha, Introduction: Third marginal ice zone research collection, *J. Geophys. Res.*, *96*, 4529-4530, 1991.

Muench, R. D., D. C. Smith IV, and C. A. Paulson, Convection beneath freezing leads: New observations compared with numerical model results, *J. Geophys. Res.*, this issue.

Pacanowski, R. C., K. Dixon, and A. Rosati, The GFDL modular ocean model users guide, version 1.0, *GFDL Ocean Group Tech. Rep., No. 2*, 1991.

Pacanowski, R. C., and S. G. H. Philander, Parameterization of vertical mixing in numerical models of the tropical oceans, *J. Phys. Oceanogr.*, *11*, 1443-1451, 1981.

Paulson, C. A., and J. D. Smith, The AIDJEX Lead Experiment, in *AIDJEX Bull. 23*, Univ. of Wash., Seattle, pp. 1-8, 1974.

Schaus, R. H., and J. A. Galt, A thermodynamic model of an arctic lead, *Arctic*, *26*, 208-221, 1973.

Smith, W. O., Jr. (Ed.), *Polar Oceanography, Part A, Physical Science*, 350 pp., Academic, San Diego, Calif., 1990.

Smith, S. D., R. D. Muench, and C. H. Pease, Polynyas and leads: An overview of physical processes and environment, *J. Geophys. Res.*, *95*, 9461-9479, 1990.

Smith, D. C., IV, and J. H. Morison, A numerical study of haline convection beneath leads in sea ice, *J. Geophys. Res.*, *98*, 10,069-10,083, 1993.

Untersteiner, N. (Ed.), *The Geophysics of Sea Ice*, 656 pp., Plenum, New York, 1986.

Ushio, S., and M. Wakatsuchi, A laboratory study on supercooling and frazil ice production processes in winter coastal polynyas, *J. Geophys. Res.*, *98*, 20,321-20,328, 1993.

Yaglom, A. M., and B. A. Kader, Heat and mass transfer between a rough wall and turbulent fluid at high Reynolds and Peclet numbers, *J. Fluid Mech.*, *62*, 601-623, 1974.

L. H. Kantha, Department of Aerospace Engineering Sciences and Program in Atmospheric and Oceanic Sciences, University of Colorado, Campus Box 431, Boulder, CO 80309-0431. (e-mail: kantha@boulder.colorado.edu)

(Received January 14, 1994; revised August 9, 1994;
accepted August 12, 1994.)